Binding of potential antitumor Casiopeínas® with small proteins†

Federico Pisanu,[a] Giuseppe Sciortino,[b] Feliu Maseras,[c] Valeria Ugone,[d] Daniele Sanna*[d] Eugenio Garribba*[a]

[a] *Dipartimento di Medicina, Chirurgia e Farmacia, Università di Sassari, Viale San Pietro, I-07100 Sassari, Italy. E-mail:* garribba@uniss.it

[b] *Departament de Química, Universitat Autònoma de Barcelona, 08193 Cerdanyola del Vallés, Barcelona, Spain*

[c] *Institute of Chemical Research of Catalonia (ICIQ), The Barcelona Institute of Science and Technology (BIST), 43007 Tarragona, Spain*

[d] *Istituto CNR di Chimica Biomolecolare, Trav. La Crucca 3, I-07100 Sassari, Italy. E-mail:* daniele.sanna@cnr.it

† Electronic Supplementary Information (ESI) available. See DOI: https://doi.org/10.1039/xxxx.

Abstract

Casiopeínas® are a family of patented Cu^{II} anticancer compounds. Cas II-gly and Cas VII-gly are formed by 4,7-dimethyl-1,10-phenanthroline (Me_2phen) or 1,10-phenanthroline (phen), respectively, and the bidentate glycinato ligand (Gly), plus a nitrate anion acting as a counterion. In biological fluids, they can keep their identity or form mixed species and adducts with several bioligands, in particular with proteins. In this study, the binding of Cas II-gly, and Cas VII-gly for comparison, to small proteins like myoglobin (Mb), ubiquitin (Ub), and lysozyme (Lyz) was evaluated through combination of instrumental (ESI-MS and EPR) and computational (dockings) methods. Simulations of the peak signals in the ESI-MS spectra allow confirming the formation of the adducts. The results indicated that in all systems adducts with formula Protein–$[Cu^{II}(Me_2phen)]_n$ with n = 1-3 are formed after the replacement of glycinato in the equatorial positions by side-chain donors. Dockings shows that the three proteins use different donor sets to bind the fragment $Cu^{II}(Me_2phen)^{2+}$: (N_{His}, N_{His}) or (N_{His}, $COO^-_{Asp/Glu}$) for Mb, N_{His68} or ($COO^-_{Glu/Asp}$, $COO^-_{Glu/Asp}$) for Ub, ($COO^-_{Glu/Asp}$, CO) or only monodentate O donor for Lyz. The computational exploration of the protein structure reveals that more than one metal fragment can bind to the macromolecule. At the moment, it is not clear whether the formation of the adducts improves or worsens the action of Casiopeínas®. However, the obtained results suggest that, at the low copper concentrations found in the organism, the species Protein–$[Cu^{II}(Me_2phen)]_n$ coexist with $[Cu^{II}(Me_2phen)(Gly)]^+$ and the fragment $Cu^{II}(Me_2phen)^{2+}$ which – in turn – could dissociate, at least partially, to Cu^{2+} ion and free ligand Me_2phen. Therefore, a mixture of species could be responsible of the biological activity of Casiopeínas®.

Keywords

Copper complexes, antitumor compounds, proteins, adduct formation, computation

Introduction

Cancer is the leading cause of death worldwide, responsible of one every six deaths and of *ca*. 10 million deaths in 2020, the most common forms being the cancer to breast, lung, colon, rectum and prostate.[1] For this reason, part of research in chemistry, pharmacy and medicine is directed toward the synthesis of new compounds for the treatment of these diseases. Among the potential anticancer drugs, metallocompounds have gained wide space in experimentation after the discovery of cisplatin.[2] The major problems of many metal-based drugs are the possible occurrence of toxic side effects, the chemoresistance due to the extended use, the unspecific action and the unclear mechanism, which often limit their applicability and clinical experimentation. To overcome these drawbacks, during the last decades many new compounds have been proposed, containing less toxic metals than Pt and platinum-group elements (PGE).

Among the most promising metals, copper (Cu) is worth being mentioned. Indeed, it is an essential element, involved in many biological processes, such as heme synthesis, cellular respiration, redox and oxygenation reactions, and electron transfer.[3] The interest for potential use of copper in medicine has recently increased and several compounds have been tested, both *in vitro* and *in vivo*, as potential anticancer drugs.[4] Some of these compounds are more effective than cisplatin on several cell lines,[4e] and may replace or integrate it, bypassing the side effects and resistance phenomena due to its prolonged administration.[4e, 5] For example, the Cu^{II} complexes formed by tridentate salphen-like ligands have an action on the HeLa cancer cells comparable to cisplatin and superior to carboplatin,[6] the compound of Cu^{II} and triapine is effective against many types of tumor cell lines,[7] while the species Cu^{II}–elesclomol, with elesclomol being the bianionic ligand derived from *N*-malonyl-bis(*N*-methyl-*N*-thiobenzoyl hydrazide), was tested for the possible treatment of metastatic melanoma.[7a]

Up to today, several Cu compounds have entered clinical trials. The combination of free copper or of copper–gluconato with disulfiram, where disulfiram is tetraethylthiuram disulfide, was suggested for the treatment of glioblastoma multiform (phase II, NCT03363659),[7a, 8] metastatic breast cancer (phase II, NCT03323346) and metastatic pancreatic tumor (phase II, NCT03714555); the complex formed by Cu^{II} and ATSM, where ATSM is diacetyl-bis(4-methyl-3-thiosemicarbazone), reached phase II for the use against rectal cancer (NCT03951337),[9] and phase II/III (NCT04082832) for the treatment of neurodegenerative disease amyotrophic lateral sclerosis;[10] the species of $^{64}Cu^{II}$ and DOTA, with DOTA being 2,2′,2″,2‴-(1,4,7,10-tetraazacyclododecane-1,4,7,10-tetrayl)tetraacetic acid, entered phase I of the trials (NCT02708511) for the positron emission tomography of patients having ovarian and breast cancer;[11] moreover, the complex of Cu^{II} and histidinato reached the phase I/II for its use against Menkes disease (NCT00001262).

Casiopeínas® are a family of very interesting compounds, with general formula $[Cu^{II}(L^{N-N})(L')]^+$, where L^{N-N} is a heterocyclic aromatic ligand such as 1,10-phenanthroline (phen) or 2,2'-bipyridine (bipy) and substituted analogs (e.g., 4,7-diphenyl-1,10-phenanthroline (Ph_2phen), 4,7-dimethyl-1,10-phenanthroline (Me_2phen), 3,4,7,8-tetramethyl-1,10-phenanthroline (Me_4phen), or 4,4'-dimethyl-2,2'-bipyridine (Me_2bipy)), and L' is a monoanionic and not or little toxic ligand like an amino acid, acetylacetone (acac), or salicylaldehyde.[12] They have been patented,[13] and the compound abbreviated with Cas III-ia, i.e., $[Cu^{II}(Me_2bipy)(acac)]^+$, is undergoing phase I of the clinical trials in Mexico.[14] Among the Casiopeínas®, $[Cu^{II}(Me_2phen)(Gly)]^+$ (Cas II-gly) and $[Cu^{II}(phen)(Gly)]^+$ (Cas VII-gly) are very promising and worthy of being mentioned; they are represented in Scheme 1. In the solid state, their structure goes from the square plane to the square pyramid and distorted octahedron, depending on the presence of the counter ion or water molecules in the axial positions.[15] Quantitative structure-activity relationships (QSAR) suggested that a crucial role is exerted by their redox behavior, the nature, number, and position of the substituents on the heterocycle – which also influences the solubility of the complexes –, and by the identity of L' ligand.[12, 16] Cas II-gly, $[Cu^{II}(Me_2phen)(Gly)]^+$, is often used as a benchmark to study their behavior in organism and biological fluids.

Casiopeínas® have been tested on various cancer cell lines, including MCF-7 (breast cancer) and HCT-15 (colon cancer), two of the most common cancer forms, and the IC_{50} values were around few μM.[12] For example, IC_{50} of $[Cu^{II}(Me_2phen)(acac)]^+$ are 4.9 and 2.1 μM on MCF-7 and HCT-15 cells,[16] to be compared with the values of 5.6 and 21.8 μM of cisplatin. From these considerations, it is clear that Casiopeínas® deserve to be further studied and developed. One problem related to their development is the lack of certain information on mechanism of action which could involve the formation of ROS, the direct interaction with DNA and mitochondrial toxicity.[12] Another key point is the transport in biological fluids, where Casiopeínas® can interact with various potential bioligands with low molecular mass (lmm) like amino acids, citrate, lactate, organic and inorganic phosphates and high molecular mass such as proteins.

A study of the ternary systems containing Cas II-gly or Cas III-Ea and of the quaternary systems with important blood and cellular bioligands (indicated generically with bL) by spectroscopic (EPR and ESI-MS) and computational (DFT) methods was recently performed.[17] The bioligands considered were citric, L-lactic acid, and L-histidine among those of serum and GSH, NADH, ATP, and L-ascorbic acid among those of cytosol. The results indicated that in all the systems mixed-ligand species Cu^{II}–Me_2phen–bL are formed, with the bioligands replacing completely or partly the glycinato ligand. With amino acids, a mixture of mixed-ligand complexes with donor set (N_{phen}, N_{phen}); (NH_2, COO^-) was formed, while with GSH, NADH and ascorbate, a redox reaction with the

partial oxidation of bioligand to GSSG, NAD^+ and dehydroascorbate and formation of Cu^I was revealed.[17]

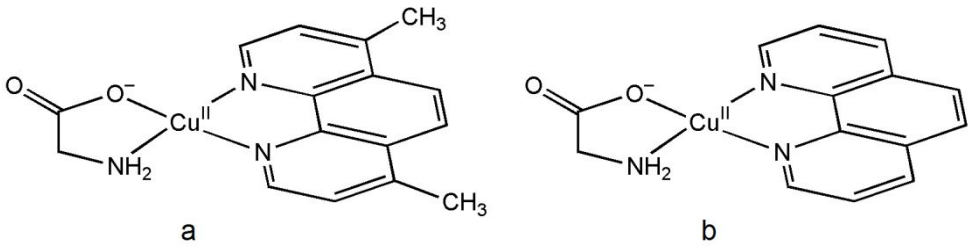

Scheme 1. Structure of the Casiopeínas® with high pharmacological activity studied in this work: (a) $[Cu^{II}(Me_2phen)(Gly)]^+$ (Cas II-gly); (b) $[Cu^{II}(phen)(Gly)]^+$ (Cas VII-gly). The water and NO_3^- ligands eventually bound to Cu^{II} ion in the axial position have been omitted for clarity.

Proteins as ceruloplasmin, albumins, transferrin, immunoglobulins, and hemoglobin can interact with Casiopeínas® as they stand or with their decomposition products. In particular, in biological fluids the initial species $[Cu^{II}(L^{N-N})(L')]^+$, and the fragments $[Cu^{II}(L^{N-N})(H_2O)_x]^{2+}$ and/or $[Cu^{II}(L')(H_2O)_x]^+$ could be generated and Protein–Cu^{II}–L^{N-N}/L' adducts could be formed in the presence of a generic protein. Similar reactions, common to other metal ions, were reviewed over the few last years for various metal and vanadium compounds.[18,19] Costa-Pessoa and coworkers demonstrated that, in aqueous solution, Casiopeínas® can bind to human serum albumin (HSA), generating a series of adducts such as HSA–Cu^{II}, HSA–$[Cu^{II}(Me_2phen)]$, and HSA–$[Cu^{II}(Me_2phen)(Gly)]$.[20] However, due to the considerable complexity of the systems, especially related to the size of HSA, which possesses various strong and weak sites, the exact composition, the type of interaction – covalent or non-covalent –, the residues involved in the binding and the three-dimensional structure of the adducts as well as their possible stabilization through secondary forces remain unclear.

In this study the binding of Cas II-gly (Scheme 1) with small model proteins, such as myoglobin (Mb), ubiquitin (Ub), and lysozyme (Lyz), that can be explored more easily than HSA or human serum transferrin (HTf) with the usual spectroscopic and computational techniques, was carried out. In some systems, the behavior of Cas VII-gly (Scheme 1), formed by phen instead of Me_2phen, was investigated for comparison. All the three proteins have been very frequently used as models for metalation studies for limited number of residues and binding sites, high purity and knowledge of the amino acid sequence.[21, 22, 23, 24]

Myoglobin is a small protein made up by 153 amino acid residues and a heme prosthetic group, with the role of transporting and storing molecular oxygen in skeletal and cardiac muscles, with

70% – under physiological conditions – folded in eight α helices (namely, A-H).[25] It is expressed in renal and prostate cell carcinoma, and for this reason has been proposed as a marker for hypovascularized tumors, particularly during the hypoxia phase.[26] During the last few years, it has been extensively used as a model protein to investigate the interaction between proteins and metal compounds.[21, 22, 27]

Ubiquitin is a little regulatory protein composed by 76 amino acid residues, with a molecular mass of about 8.5 kDa.[21-22, 28] Like myoglobin, it has been exploited as model for the interaction with proteins of anticancer metallocompounds containing platinum,[29] ruthenium,[30] and vanadium.[31] It shows only few potential metal binding sites, the *N*-terminal methionine, Met1 (S-donor), His68 (N-donor), and a certain number of kinetically favored O-donor residues, especially carboxylates.[28]

Lysozyme is a protein with 129 amino acids and a molecular mass of 14.3 kDa,[22] which behaves as a glycoside hydrolase, catalyzing the hydrolysis of 1,4-β bond between *N*-acetylmuramic acid and *N*-acetyl-D-glucosamine in peptidoglycan,[32] and has an important relevance in animals in the processes of host defense processes.[33] Similarly to Mb and Ub, it has been used as a model protein for the binding of Pt-, Ru-, Rh- and Au-based drugs.[23-24, 34, 35]

The use of models proteins to study metal binding is valuable for several reasons:[21-24, 34-35] i) they allow to control specific variables, such as amino acid composition, sequence or binding motifs, simplifying significantly the study of the interaction mechanisms; ii) structural information can be more easily obtained because it is possible to focus on specific binding domains or structural motifs without the interference from multifunctional regions in larger proteins; iii) they often have well-characterized and predictable properties, making it easier to interpret results and compare them to theoretical or computational models; iv) well-defined and simple model systems reduce experimental variability, leading to more reproducible results; v) specific binding sites, mutations, or modifications to test hypotheses about how certain features (e.g., side-chains, metal environment, and coordination geometry) influence metal binding can be easily designed; vi) they often derive from physiologically relevant proteins (e.g., myoglobin is the monomer of hemoglobin), providing general insights into how these latter interact with metals in processes like medicinal action, enzymatic catalysis, electron transfer, or metal detoxification; vii) they can be easily studied with instrumental techniques (e.g., X-ray crystallography, Nuclear Magnetic Resonance (NMR) and Electron Paramagnetic Resonance (EPR) spectroscopy) due to their smaller size and reduced complexity. Therefore, by focusing on model proteins, research can develop fundamental knowledge about metal-protein interactions, which can later be applied to understand and interpret more complex systems in biological and medicinal contexts.

With Mb, Ub, and Lyz the interaction Casiopeínas®-protein is related to the sites available and stability of the formed adducts, and can be covalent or non-covalent, depending on the possible replacement of glycinato or Me_2phen/phen to give the fragments $[Cu^{II}(L^{N-N})(H_2O)_x]^{2+}$ or $[Cu^{II}(L')(H_2O)_x]^{+}$, to which one or two side-chain donors can bind. The adducts could have high importance in the biological and pharmacological activity and the results may provide new insights on the interaction of Casiopeínas® with the other proteins of biofluids and information on the formation of the active species in organism and their action mode. The study was carried out using a combined application of instrumental techniques (ElectroSpray Ionization-Mass Spectrometry (ESI-MS) and EPR) and computational methods (docking and density functional theory (DFT) calculations) that could be successfully applied to other metal-containing systems.

Experimental and computational details

Materials

Water was deionized prior to use through the purification system Millipore Milli-Q Academic for EPR or purchased with LC-MS grade (Sigma-Aldrich, code 1.15333) for ESI-MS measurements. LC-MS grade methanol (MeOH) (Sigma-Aldrich, code 1.06035) was used in 10% (v/v) mixture with LC-MS water, for ESI-MS measurements. Glycine (Gly; Merck, code 4201), 4,7-dimethyl-Glycine (Gly; Merck, code 4201), 4,7-dimethyl-1,10-phenanthroline (Me_2phen; Sigma-Aldrich, code 301809; Alfa Aesar A17779), phenanthroline (phen; Sigma-Aldrich, code 00615KW), 1-methylimidazole (MeIm; Sigma-Aldrich, code M50834), 3-(*N*-morpholino)propanesulfonic acid (MOPS; Across Organics, code 172630250), $(NH_4)_2CO_3$ (Carlo Erba, code 419237), myoglobin from equine heart (Mb; Sigma-Aldrich, code M1882), ubiquitin from bovine erythrocytes (Ub; Sigma-Aldrich, code U6253), lysozyme from chicken egg white (Lyz; Sigma-Aldrich, code 62970). For EPR measurements, $^{63}CuSO_4 \cdot 5H_2O$ was synthesized from metallic ^{63}Cu with an isotopic purity of 99.9% purchased from Cambridge Isotope Laboratories, Inc. For ESI-MS measurements, $CuCl_2$ (Sigma-Aldrich, code 222011) was used. Finally, H_2SO_4 (96% v/v), HNO_3 (65% v/v) and HCl (37% v/v), $(NH_4)_2CO_3$, and NaOH as pellets, all purchased from Carlo Erba, were also employed to change pH values.

All the compounds were used as received.

ESI-MS measurements and mass spectra analysis

Solutions for ESI-MS measurements were prepared either in pure LC-MS solvent. Water or

MeOH/H_2O 10/90 (v/v) mixtures were used, with a copper to protein ratio in the range 1/1-5/1 and a protein concentration of 0.5, 5 or 50 μM. The initial pH of each system, in the range 2-3, was brought as close as possible to the neutral value, generally between 6.5 and 7.0 with $(NH_4)_2CO_3$. Subsequently, the solutions were diluted to 5 or 50 μM to record the mass spectra.

Positive-ion mode ESI-MS (ESI-MS(+)) spectra were recorded with a high-resolution Q Exactive™ Plus Hybrid Quadrupole-Orbitrap™ mass spectrometer (Thermo Fisher Scientific). The solutions were infused at a flow rate of 5.00 μL/min into the ESI chamber. Spectra were recorded in the m/z range 50-1000 with a resolution of 140000. ESI-MS(+) spectra were recorded using the following instrumental conditions: spray voltage 2300 V, capillary temperature 250 °C, sheath gas 5-10 (arbitrary units), auxiliary gas 3 (arbitrary units), sweep gas 0 (arbitrary units), probe heater temperature 50 °C. All the mass spectra were analyzed by using Thermo Xcalibur 3.0.63 software (Thermo Fisher Scientific). The average deconvoluted monoisotopic masses were obtained with the software Unidec 4.4.0,[36] the deviation from the expected masses being 2-3 Da.

The simulated peaks of the mass spectra for selected charge states (*z*) of the free proteins and their adducts with the fragments $Cu^{II}(Me_2phen)^{2+}$ and $Cu^{II}(phen)^{2+}$, deriving from Cas II-gly and Cas VII-gly, respectively, were obtained using the Mass Spectrum Simulator tool of Prot pi,[37] an online "free-to-use bioinformatic tool box" developed in collaboration with the Center for Biochemistry and Bioanalytics at Zurich University of Applied Sciences. The program allows generating simulated mass spectra for a given neutral molecular formula, which can be charged by a selectable number of cations or anions, *e.g.,* H^+, Na^+, K^+, NH_4^+, or $Cl^–$, $Br^–$, $HCOO^–$, and more. In this work, the neutral molecular formula for each protein was calculated from the protein sequence by summing the molecular formula of the amino acids (in their neutral form) and by subtracting an equivalent of H_2O for each peptide bond and an equivalent of H_2 for each disulfide bridge. The program also allows considering the resolution of the peaks (the resolution used for all the simulations was 70000, the value which best fitted the shape of the experimental peaks).

In the case of myoglobin, due to the presence of the prosthetic group, heme b, two forms, apo-Mb and holo-Mb, must be considered. The sequence of apo-Mb, from *Equus caballus* (horse), was obtained from UniProt, ID P68082, and consists of 155 amino acid residues, from which the first one, Met1, was discarded to obtain the mature sequence of 154 residues.[38] The neutral molecular formula of apo-Mb resulted $C_{769}H_{1212}N_{210}O_{218}S_2$. To obtain the molecular formula for holo-Mb, the formula of the neutral heme b ($C_{34}H_{32}Fe^{II}N_4O_4$) with Fe in the oxidation state +2, was added to apo-Mb. A good agreement between experimental and simulated spectra of holo-Mb was obtained considering a monocationic and not a neutral form of the prosthetic group, with the iron oxidation state +3 instead of +2, as observed in other studies with myoglobin;[39] this is probably due to the

oxidation of Fe^{II} to Fe^{III} in the ESI chamber during the recording of the spectrum.[40] In this way, the formula for holo-Mb corresponds to the monocation $C_{803}H_{1244}Fe^{III}N_{214}O_{222}S_2^+$.

The neutral formula calculated for ubiquitin was derived from the sequence of polyubiquitin C of *Bos taurus* (bovine) and results $C_{378}H_{629}N_{105}O_{118}S$. This sequence (UniProt ID P0CH28) consists of 690 amino acid residues, namely the sequence of monoubiquitin (76 residues[41]) repeated for nine times plus a small sequence of six residues (Val-Leu-Ser-Ser-Pro-Phe) at the *C*-terminus. Accounting for this, only the first 76 residues of the sequence were considered for Ub.

The sequence of lysozyme C from *Gallus gallus* (chicken), with UniProt ID P00698, was used to calculate the neutral molecular formula of the protein. The sequence presents a total of 147 residues, of which the first 18 residues were discarded to obtain the mature primary structure of 129 residues.[42] Moreover, four disulfide bridges were considered, resulting in the neutral molecular formula $C_{613}H_{951}N_{193}O_{185}S_{10}$.

EPR measurements

Solutions for EPR measurements were prepared mixing appropriate amounts of copper and proteins to obtain a ratio from 1/1 to 5/1 and a final Cu^{II} concentration of 1.0×10^{-3} M. The pH values of the solutions were varied with diluted solutions of H_2SO_4 and NaOH. The spectra were recorded from pH 3.0 to 9.0, paying particular attention that at least one of them was in the pH range 7.2-7.6, i.e. close to the physiological pH. MOPS was employed as a buffer to reach a pH of 7.4.

EPR spectra were recorded immediately after the preparation of the solutions at 120 K with an X-band Bruker EMX spectrometer equipped with a HP 53150A microwave frequency counter and a variable temperature unit. The microwave frequency was 9.40-9.41 GHz, microwave power was 20 mW (which is, with the ER4119 HS resonator, below the saturation limit), time constant 81.92 ms, modulation frequency 100 kHz, modulation amplitude 0.4 mT, resolution 4096 points.

DFT calculations

The structure of $[Cu^{II}(Me_2phen)(H_2O)_2]^{2+}$ was optimized with Gaussian 16 software (revision *B.01*)[43] at DFT theory level. The hybrid Becke three-parameters B3LYP-D3 functional,[44] with the Grimme's D3 correction for dispersion,[45] was used combined with the split-valence Pople basis set 6-31g(d,p) for the main group elements, while Stuttgard-Dresden (SDD) implemented with *f*-functions and pseudo-potential was applied for Cu. These computational conditions were successfully employed for the geometry prediction of first-row transition metal complexes.[46] Geometry optimizations were carried out in water with the SMD model [47] and minima were verified through frequency calculations. The atomic coordinates of $[Cu^{II}(Me_2phen)(H_2O)_2]^{2+}$ are available in

Table S1 of the Electronic Supplementary Information (ESI) and in the ioChem-BD repository.[48]

Docking calculations

Docking calculations were carried out with software GOLD version 5.3.[49] Initially, the receptor proteins, myoglobin (PDB code: 4DC8 [50]), ubiquitin (3H1U [51]), and lysozyme (2LYZ [52]), were prepared removing all possible small species or water molecules with the program UCSF Chimera.[53] The metal complex fragments, $Cu^{II}(Me_2phen)^{2+}$ or $Cu^{II}(Me_2phen)(H_2O)^{2+}$, derived from Cas II-gly after the release of the glycinato ligand, were DFT-optimized as $[Cu^{II}(Me_2phen)(H_2O)_2]^{2+}$ using the functional B3LYP-D3 as described above.

The interaction between the fragment $Cu^{II}(Me_2phen)^{2+}$ was studied by 'activating' the equatorial water molecules with dummy hydrogen atoms, as established in the literature.[54] The structure of each protein was explored with BioMetAll software,[55] searching for zones containing a minimum of two coordinating amino acids, whose types should be a combination of His, Asp, Glu, Met, Asp, Gln and Asn: (His, His), (His, Met/Asp/Glu/Gln/Asn) or (Asp/Glu, Met/Asp/Glu/Gln/Asn). The regions that met these criteria were subsequently evaluated by docking calculations.

In the calculations, the possible protonation of the nitrogen atoms on the imidazole ring of histidine residues at δ or ε was considered; in particular, in each simulation, one of the two nitrogens was protonated. The docking simulations were performed by constructing a 12 Å evaluation sphere in the region of interest, taking into account the flexibility of the side-chains using the rotamer libraries implemented by GOLD.[56] The genetic algorithm (GA) parameters were set at 50 runs GA and a minimum of 100000 operations. All other GA parameters were left as default. The solutions were analyzed using GaudiView.[57] Scoring (GoldScore Fitness) was evaluated using the modified version of the GoldScore scoring function, in accordance with the published data.[54b] For each system, the 50 docking solutions, one per GA run, were clustered in docking poses within a root mean square deviation (RMSD) value of 2.5 Å, each cluster representing a pose. Every solution was evaluated by the associated GoldScore Fitness parameter, F, and each pose was estimated taking into account the mean (F_{mean}) and highest (F_{max}) F value of the associated cluster.

Results and discussion

Systems Cu^{II}/Me_2phen, $Cu^{II}/Me_2phen/Gly$ and $Cu^{II}/Me_2phen/MeIm$

To understand if either the glycinato ligand of Cas II-gly remains bound to the Cu^{II} center in solution or it can be replaced by bioligands like proteins, the anisotropic EPR spectra of the binary

Cu^{II}/Me_2phen system in MOPS at various pH values were recorded.

At pH around 4, only the species $[Cu^{II}(Me_2phen)(H_2O)_2]^{2+}$ (indicated with **I** in trace a of Fig. 1) is observed in solution, with a very small amount of the signals of aquaion $[Cu^{II}(H_2O)_6]^{2+}$ (indicated with **aq**); $[Cu^{II}(Me_2phen)(H_2O)_2]^{2+}$ is characterized by g_z = 2.308 and A_z = 168.5 × 10^{-4} cm^{-1}. As pH is increased to the physiological value, the formation of a di-μ-hydroxido complex, $[Cu^{II}_2(Me_2phen)_2(OH)_2(H_2O)_2]^{2+}$, is observed (**II** in trace b of Fig. 1); its spectrum is characterized by two peaks in the $\Delta M = \pm 1$ region, falling at 288.3 mT and 361.1 mT and spaced of 72.8 mT around *g ca*. 2.1. Similarly to the spectrum of the complex formed by a structurally similar ligand, 2,2'-bipyridine (bipy), with formula $[Cu^{II}_2(bipy)_2(OH)_2]^{2+}$, the two signals could be attributed to the perpendicular resonances;[58] the *g* factor is 2.070 and the calculated zero-field splitting *D* is 0.0704 cm^{-1}. From the spin Hamiltonian parameters and postulating that *D* has only a dipolar origin without contributions from anisotropic exchange, the value of *R*, the distance between the two Cu^{2+} centres, can be calculated with the equation proposed by Stevens,[59] $D = [0.325g^2 \times |1 - 3\cos^2\theta|] / R^3$, with *D* in cm^{-1} and *R* in Å. Using the value of *ca*. 95° for the angle θ formed by the Cu–OH_2 and Cu–Cu directions of the crystallographic structure of $[Cu^{II}_2(phen)_2(OH)_2(H_2O)_2]^{2+}$,[60] the calculated value of *R* is around 2.7 Å, in good agreement with that experimental for the dinuclear structure formed by 1,10-phenanthroline (2.9 Å).

This means that, around neutrality, hydrolysis is significant, one of the two water molecules in $[Cu^{II}(Me_2phen)(H_2O)_2]^{2+}$ undergoes deprotonation and the hydroxido-bridged dimer is formed. As it can be discussed later, the band at 288.3 mT is very useful to differentiate the behaviour of the systems with only Me_2phen or Me_2phen plus Gly from those of the systems with proteins where such an absorption is lacking.

In the system with Gly, where the complex $[Cu^{II}(Me_2phen)(Gly)]^+$ forms (i.e., Cas II-gly), the resonances of two species are revealed: $[Cu^{II}_2(Me_2phen)_2(OH)_2(H_2O)_2]^{2+}$ (**II**) and $[Cu^{II}(Me_2phen)(Gly)]^+$ (**III** in trace c of Fig. 1). This suggest that Gly binds, at least in part, the fragment $Cu^{II}(Me_2phen)^{2+}$ but it is not strong enough to suppress the hydrolysis and formation of the di-μ-hydroxido bridged complex.

Table 1 Spin Hamiltonian EPR parameters of the complexes detected in systems Cu^{II}/Me_2phen, Cu^{II}/Me_2phen/Gly and Cu^{II}/Me_2phen/MeIm.

Complex	g_z	A_z [a]
$[Cu^{II}(Me_2phen)(H_2O)_2]^{2+}$	2.308	168.5
$[Cu^{II}(Me_2phen)(Gly)]^+$	2.248	186.1

$[Cu^{II}(Me_2phen)(MeIm)(H_2O)]^{2+}$	2.254	184.5

[a] Values given in 10^{-4} cm^{-1} units.

MeIm is a good model for simulating the coordination of a His residue to a metal ion,[61, 62] and – for this reason – the system Cu^{II}/Me_2phen/MeIm was also explored (trace d of Fig. 1). When the behavior of the system containing Cas II-gly is compared with that containing Cu^{II}/Me_2phen/MeIm, another species can be observed (**IV**) with a lower g_z value (2.254) and higher A_z (184.5×10^{-4} cm^{-1}), suggesting that one or more equatorial water molecules have been replaced by 1-methylimidazole. The fact that the EPR signals do not appreciably change increasing the amount of MeIm from 1 to 2 equivalents (cfr. traces d and e of Fig. 1) would suggest that only one 1-methylimidazole ligand binds to the Cu^{2+} ion. Moreover, at pH 7.4 the spectral intensity in the ternary system Cu^{II}/Me_2phen/MeIm, higher than in the binary one Cu^{II}/Me_2phen, and the disappearance of the band of the dimer $[Cu^{II}_2(Me_2phen)_2(OH)_2(H_2O)_2]^{2+}$, suggest that the mixed-ligand complex $[Cu^{II}(Me_2phen)(MeIm)(H_2O)]^{2+}$ is rather stable at physiological pH, keeping Cu^{2+} in solution and suppressing the hydrolytic reactions.

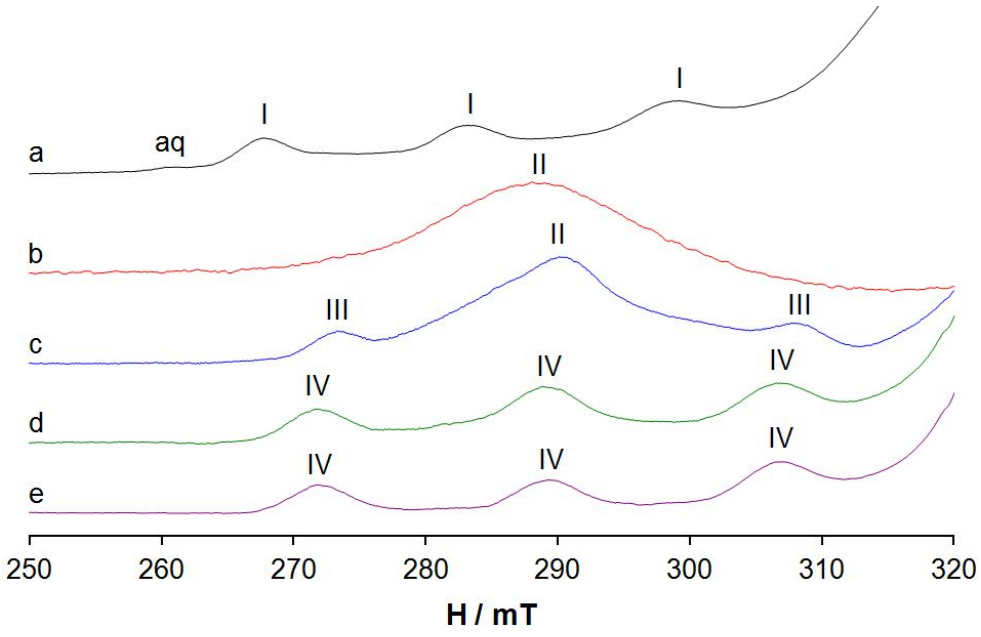

Fig. 1 Low-field region of the anisotropic X-band EPR spectra recorded as a function of pH on frozen solutions (120 K) containing: a) $^{63}Cu^{II}$/Me_2phen 1/1, pH 3.90; b) $^{63}Cu^{II}$/Me_2phen 1/1, pH 7.30; c) $^{63}Cu^{II}$/Me_2phen/Gly 1/1/1, pH 7.40; d) $^{63}Cu^{II}$/Me_2phen/MeIm 1/1/1, pH 7.10; e) $^{63}Cu^{II}$/Me_2phen/MeIm 1/1/2, pH 7.10. In all the systems, the concentrations of $^{63}Cu^{II}$ and MOPS were 1.0×10^{-3} M and 0.1 M, respectively. **I** denotes the resonances of $[Cu^{II}(Me_2phen)(H_2O)_2]^{2+}$, **II** of $[Cu^{II}_2(Me_2phen)_2(OH)_2(H_2O)_2]^{2+}$, **III** of $[Cu^{II}(Me_2phen)(Gly)]^{+}$, and **IV** of

$[Cu^{II}(Me_2phen)(MeIm)(H_2O)]^{2+}$.

3.2. Systems Cu^{II}/Mb, Cu^{II}/Me_2phen/Mb and Cas II-gly/Mb

The ESI-MS spectrum of the pure myoglobin in aqueous solution (5 μM) was recorded in positive-ion mode and showed a pattern of signals stemming from different charge states, *z*, comprised between +7 and +14, with *z* = +10 representing the most intense peaks (Fig. S1 of ESI†). The deconvoluted spectrum (Fig. S2 of ESI†) shows two sets of peaks with a mass difference of 616 Da, that is the mass of the prosthetic group, i.e. heme b;[27, 63] in other words, the two signals derive from the apo and the holo forms of protein. According to the results in the literature, the signals of holo-Mb are more intense than those of apo form, suggesting that heme group remains mainly bound to the protein under such experimental conditions.[64] The heme, lost from holo-Mb, is detected in the spectrum at m/z = 616.18; the experimental and simulated peak series are displayed in Fig. S3 of ESI†.

The ESI-MS(+) spectrum of the system Cu^{II}/Mb recorded with a molar ratio of 5/1 shows that myoglobin can form adducts with copper ions. In the deconvoluted spectrum (Fig. 2), both apo- and holo-Mb present two main peaks, one attributed to the free protein (apo-Mb at 16950 Da and holo-Mb at 17566 Da) and another to the adducts apo-Mb–[Cu^{II}] and holo-Mb–[Cu^{II}] at *ca*. +62 Da (17012 and 17628 Da, respectively) compared to the metal-free forms.

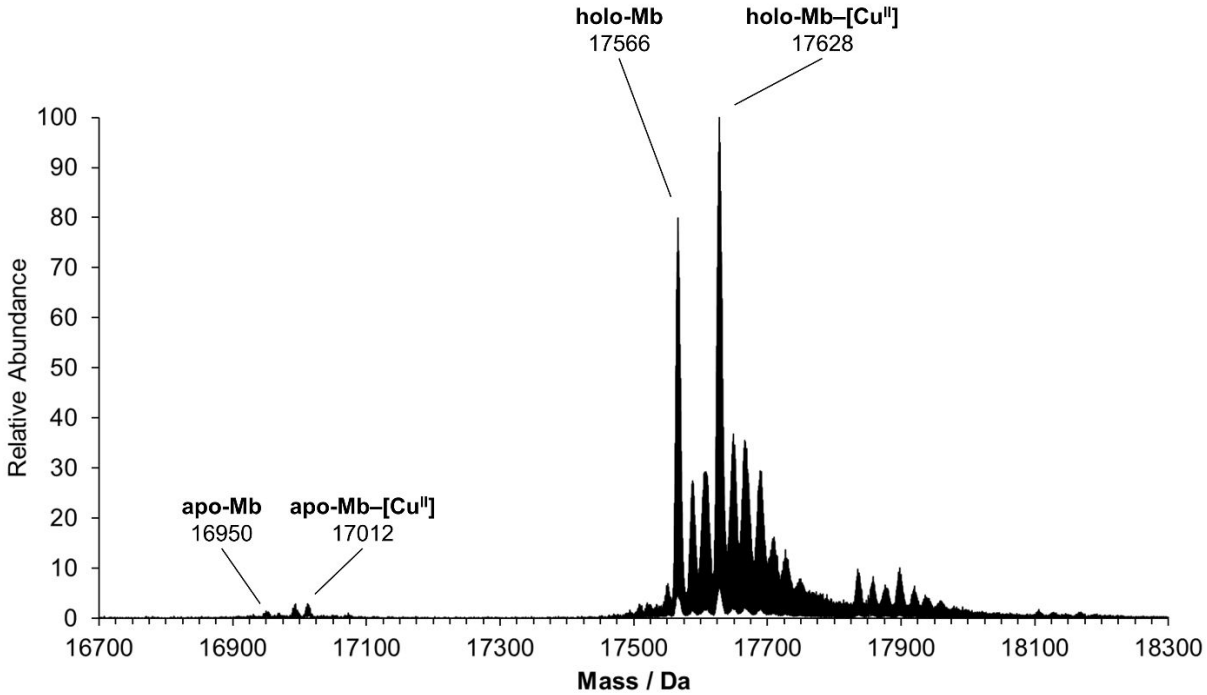

Fig. 2 Deconvoluted ESI-MS(+) spectrum of the system Cu^{II}/Mb 5/1 in H_2O. The concentration of

Mb was 5 μM.

The deconvoluted ESI-MS(+) spectrum of the system Cu^{II}/Me_2phen/Gly/Mb shows a series of peaks (Fig. 3). Those at 17675 and 17944 Da are attributed to the free holo-Mb and to its adduct with the fragment $Cu^{II}(Me_2phen)^{2+}$, respectively (Fig. 3). A mass difference around 270 Da is compatible with a $Cu^{II}(Me_2phen)^{2+}$ fragment, suggesting the formation of a holo-Mb–[$Cu^{II}(Me_2phen)$] adduct. The large number of peaks observed in correspondence of the signals of the free protein and holo-Mb–[$Cu^{II}(Me_2phen)$] species is due to the adducts with multiple Na^+ ions; indeed, each peak is separated from the neighboring ones by approximately 22 Da, i.e., the mass of a Na^+ ion minus that of a proton.

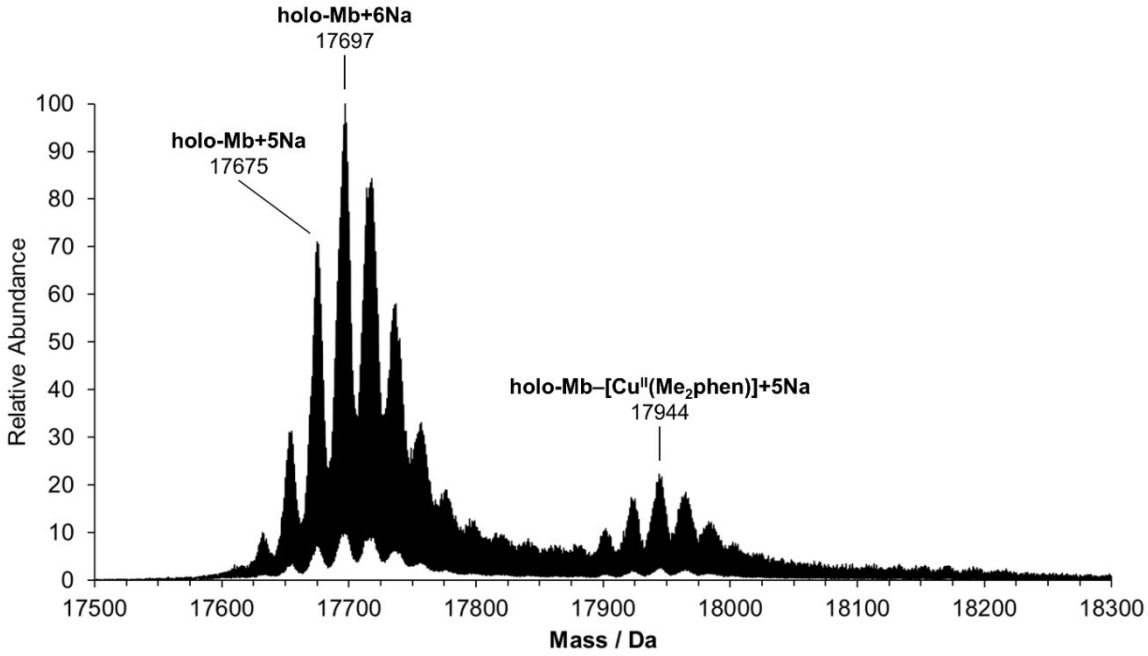

Fig. 3 Deconvoluted ESI-MS(+) spectrum of the system Cu^{II}/Me_2phen/Gly/Mb 1/1/1/1 in H_2O. The concentration of Mb was 50 μM

The comparison between the simulated and the non-deconvoluted experimental peaks of the ESI-MS(+) spectrum with z = +9, chosen for being the most intense, allowed us to confirm the attribution of the signals in the deconvoluted spectrum shown in Fig. 3. The comparison is displayed in Fig. 4. The formulae used to simulate the experimental peaks attributed to the free holo-Mb are: a) $[holo\text{-}Mb+4H+4Na]^{9+}$, b) $[holo\text{-}Mb+3H+5Na]^{9+}$, c) $[holo\text{-}Mb+2H+6Na]^{9+}$, d) $[holo\text{-}Mb+H+7Na]^{9+}$, e) $[holo\text{-}Mb+8Na]^{9+}$, f) $[holo\text{-}Mb+9Na-H]^{9+}$, where holo-Mb always stands

for $C_{803}H_{1244}Fe^{III}N_{214}O_{222}S_2^+$ as reported in the Experimental and computational section. It must be noted that holo-Mb already bears one positive charge and, thus, in the spectra simulation, the total charge +9 can be maintained by summing the total charge of the eight monocationic ions, among which H^+ and Na^+. For the formula denoted with the letter f, since $9Na^+$ were used to simulate the adduct, one positive charge must be subtracted to keep the total z = +9, this being achieved by subtracting one proton ($-H^+$). In addition, the peaks of the adduct with $Cu^{II}(Me_2phen)^{2+}$ in the m/z range 1992-2001 were also simulated with the following formulae: g) [holo-Mb–$Cu^{II}(Me_2phen)$+2H+4Na]$^{9+}$, h) [holo-Mb–$Cu^{II}(Me_2phen)$+H+5Na]$^{9+}$, i) [holo-Mb–$Cu^{II}(Me_2phen)$+6Na]$^{9+}$, j) [holo-Mb–$Cu^{II}(Me_2phen)$+7Na−H]$^{9+}$, using $C_{14}H_{12}Cu^{II}N_2^{2+}$ for the fragment $Cu^{II}(Me_2phen)^{2+}$. The comparison shows a good agreement between the signals of simulations and those experimentally observed, confirming the attribution of this series of peaks to the holo-Mb–[$Cu^{II}(Me_2phen)$] adduct.

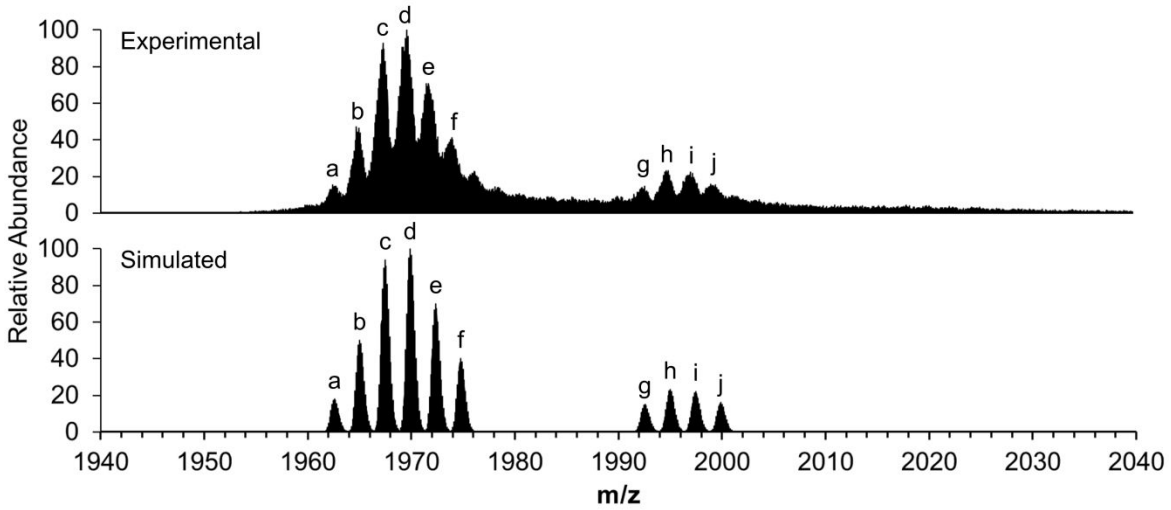

Fig. 4 Experimental (above) and simulated (below) region (m/z range 1940-2040, z = +9) of the ESI-MS(+) spectrum of the system Cu^{II}/Me_2phen/Gly/Mb 1/1/1/1 in H_2O (10% MeOH). The concentration of Mb was 50 μM. The following peaks were simulated: a) [holo-Mb+4H+4Na]$^{9+}$; b) [holo-Mb+3H+5Na]$^{9+}$; c) [holo-Mb+2H+6Na]$^{9+}$; d) [holo-Mb+H+7Na]$^{9+}$; e) [holo-Mb+8Na]$^{9+}$; f) [holo-Mb+9Na−H]$^{9+}$; g) [holo-Mb–$Cu^{II}(Me_2phen)$+2H+4Na]$^{9+}$; h) [holo-Mb–$Cu^{II}(Me_2phen)$+H+5Na]$^{9+}$; i) [holo-Mb–$Cu^{II}(Me_2phen)$+6Na]$^{9+}$; j) [holo-Mb–$Cu^{II}(Me_2phen)$+7Na−H]$^{9+}$. In all the simulations, holo-Mb stands for the holo form of myoglobin, with molecular formula $C_{803}H_{1244}Fe^{III}N_{214}O_{222}S_2^+$, while the formula of $Cu^{II}(Me_2phen)^{2+}$ is $C_{14}H_{12}Cu^{II}N_2^{2+}$.

EPR spectra were collected on the system Cu^{II}/Me_2phen/Mb at room temperature (298 K, RT) and

low temperature (120 K, LT). The spectra recorded at RT are reported in Fig. S4 of ESI†. It can be seen that, besides the isotropic resonances due to the presence of $[Cu^{II}(Me_2phen)(H_2O)_2]^{2+}$ and/or hydrolytic Cu^{II} species, the anisotropic signals (indicated with an asterisk) of the Mb–$[Cu^{II}(Me_2phen)]$ adduct were detected. This agrees well with ESI-MS results and confirms that the $Cu^{II}(Me_2phen)^{2+}$ fragment is able to interact with myoglobin with a number of protein donors which can range from 1 (one equatorial site) to 3 (two equatorial plus an axial position).

The anisotropic EPR spectra recorded at pH = 7.4 at LT, varying the molar ratio between $Cu^{II}(Me_2phen)^{2+}$ fragment and Mb, are shown in Fig. 5, traces c-e. First of all, it should be noted that the pattern of the spectra changes between the reference system with Cas II-gly (Cu^{II}/Me_2phen/Gly, trace a of Fig. 5) where **II** and **III** indicate the resonances of $[Cu^{II}_2(Me_2phen)_2(OH)_2(H_2O)_2]^{2+}$ and $[Cu^{II}(Me_2phen)(Gly)]^{+}$) and the systems with 1-methylimidazole or myoglobin; moreover, the intensity of the spectral signals in the presence of the protein is higher compared to that obtained on the system without it, i.e., Cu^{II}/Me_2phen/Gly, and this suggests that the formation of Mb–$[Cu^{II}(Me_2phen)]$ occurs, leading to a decrease or even an inhibition of the hydrolysis processes. Secondly, the position of the resonances of the species revealed with Mb (traces c-d of Fig. 5) is significantly different respect to that of $[Cu^{II}(Me_2phen)(MeIm)(H_2O)]^{2+}$ (**IV** in the trace b of Fig. 5). Thirdly, the signals observed in the system Cu^{II}/Me_2phen/Mb change slightly with the decreasing of the Mb/Cu^{II} molar ratio, probably because the number of the fragments bound to copper center is more than 1; these adducts are indicated with **Va** and **Vb** in Fig. 5 and Mb–$[Cu^{II}(Me_2phen)]^{\mathbf{a}}$ and Mb–$[Cu^{II}(Me_2phen)]^{\mathbf{b}}$ in the text. Indeed, at a closer look to the deconvoluted mass spectrum (Fig. 3), a set of peaks with very low intensity at 18100-18200 Da seems to confirm the presence of the adduct Mb–$[Cu^{II}(Me_2phen)]_2$, even if the signal to noise ratio is too low for this to be proved.

The change in the spin Hamiltonian parameters of Mb–$[Cu^{II}(Me_2phen)]^{\mathbf{a}}$ and Mb–$[Cu^{II}(Me_2phen)]^{\mathbf{b}}$ with respect to the mixed-ligand species $[Cu^{II}(Me_2phen)(MeIm)(H_2O)]^{2+}$ indicates that Mb binds to Cu^{2+} ion with donors stronger than [(N_{phen}, N_{phen}); N_{imid}; H_2O] and that, hence, the coordination for the species indicated with **Va** and **Vb** could be [(N_{phen}, N_{phen}); (N_{His}, $COO^-_{Glu/Asp}$)] and/or [(N_{phen}, N_{phen}); (N_{His}, N_{His})], as confirmed by docking calculations (see below). The spin Hamiltonian parameters are $g_z = 2.246$ and $A_z = 182.9 \times 10^{-4}$ cm^{-1} for Mb–$[Cu^{II}(Me_2phen)]^{\mathbf{a}}$ and $g_z \sim 2.24$ and $A_z \sim 185 \times 10^{-4}$ cm^{-1} for Mb–$[Cu^{II}(Me_2phen)]^{\mathbf{b}}$ (Table 2). Notably, the resonances of Mb–$[Cu^{II}(Me_2phen)]^{\mathbf{a}}$ and Mb–$[Cu^{II}(Me_2phen)]^{\mathbf{b}}$ do not coincide with those of $[Cu^{II}(Me_2phen)(Gly)]^{+}$, further supporting that the binding mode of myoglobin is different from (NH_2, COO^-). The possibility that there are additional signals from other binding sites, covered by the broad resonances of the two adducts, cannot be ruled out.

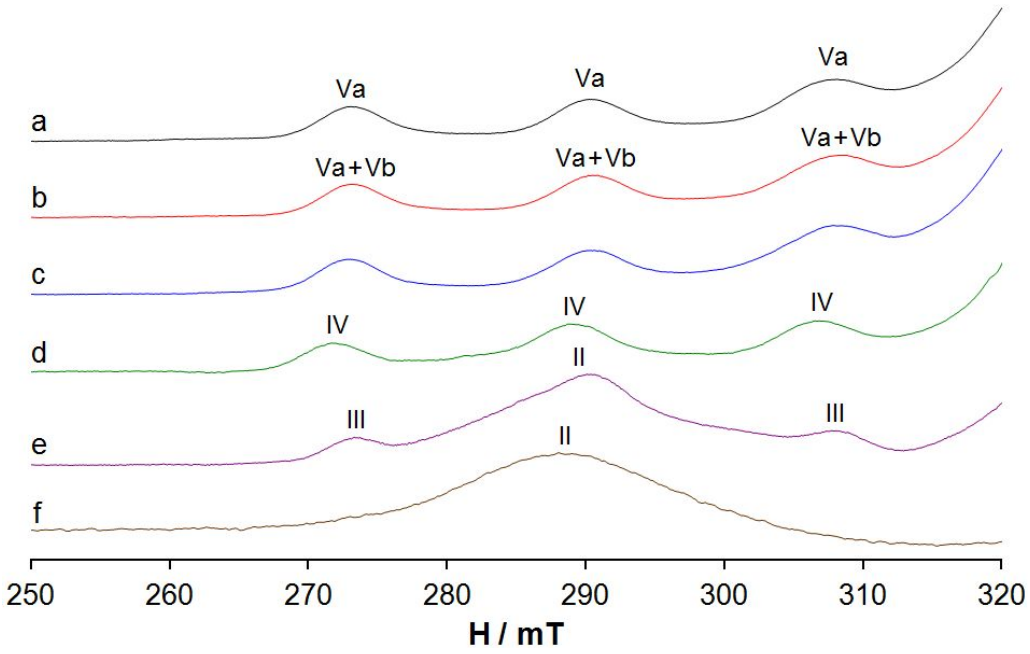

Fig. 5 Low-field region of anisotropic X-band EPR spectra recorded at pH 7.40 on frozen solutions (120 K) containing: a) $^{63}Cu^{II}$/Me_2phen/Mb 1/1/1; b) $^{63}Cu^{II}$/Me_2phen/Mb 2/2/1; c) $^{63}Cu^{II}$/Me_2phen/Mb 4/4/1; d) $^{63}Cu^{II}$/Me_2phen/MeIm 1/1/1; e) $^{63}Cu^{II}$/Me_2phen/Gly 1/1/1; f) $^{63}Cu^{II}$/Me_2phen 1/1. In all the systems, the concentrations of $^{63}Cu^{II}$ and MOPS were 1.0×10^{-3} M and 0.1 M, respectively. **II**, **III**, **IV**, **Va** and **Vb** denote the resonances of the species $[Cu^{II}_2(Me_2phen)_2(OH)_2]^{2+}$, $[Cu^{II}(Me_2phen)(Gly)]^{+}$, $[Cu^{II}(Me_2phen)(MeIm)(H_2O)]^{2+}$ and of the two adducts Mb–$[Cu^{II}(Me_2phen)]^{\mathbf{a}}$ and Mb–$[Cu^{II}(Me_2phen)]^{\mathbf{b}}$.

Table 2 Spin Hamiltonian EPR parameters of the complexes of the adducts formed by Cas II-gly with the studied proteins.

Complex / adduct	g_z	A_z [a]	Proposed equatorial donors [b]
$[Cu^{II}(Me_2phen)(Gly)]^{+}$	2.248	186.1	(NH_2, COO^-)
Mb–$[Cu^{II}(Me_2phen)]^{\mathbf{a}}$ [c]	2.246	182.9	(N_{His}, $COO^-_{Glu/Asp}$) or (N_{His}, N_{His})
Mb–$[Cu^{II}(Me_2phen)]^{\mathbf{b}}$ [d]	~ 2.24	~ 185	(N_{His}, $COO^-_{Glu/Asp}$) or (N_{His}, N_{His})
Ub–$[Cu^{II}(Me_2phen)]^{\mathbf{a}}$ [e]	~ 2.27	~ 176	($COO^-_{Glu/Asp}$, $COO^-_{Glu/Asp}$)
Ub–$[Cu^{II}(Me_2phen)]^{\mathbf{b}}$ [f]	~ 2.25	~ 181	N_{His}; H_2O
Lyz–$[Cu^{II}(Me_2phen)]^{\mathbf{a}}$ [g]	~ 2.25	~ 174	($COO^-_{Glu/Asp}$, CO)

[a] Values reported in 10^{-4} cm^{-1} units. [b] For Me_2phen the equatorial donors are (N_{phen}, N_{phen}) in all cases. [c] **Va** in Figs. 5 and 6. [d] **Vb** in Figs. 5 and 6. [e] **VIa** in Figs. 6 and 11. [f] **VIb** in Figs. 6 and 11. [g] **VII** in Figs. 6 and 15.

In Fig. 6, the comparison of the spectra obtained with Cas II-gly (system Cu^{II}/Me_2phen/Gly), 1-methylimidazole, and the three proteins studied in this work (myoglobin, ubiquitin, and lysozyme) is presented. Concerning Mb, it can be observed that the position of the absorptions of Mb–$[Cu^{II}(Me_2phen)]^{a}$ and Mb–$[Cu^{II}(Me_2phen)]^{b}$ (**Va** and **Vb** in Fig. 6) is similar but not coincident with that of $[Cu^{II}(Me_2phen)(Gly)]^{+}$ (**III** in Fig. 6) which has (N_{phen}, N_{phen}); (NH_2, COO^{-}) coordination mode. This confirms that the donors have similar but not equal strength, as shown by the spin Hamiltonian parameters in Table 2 and docking calculations (see below).

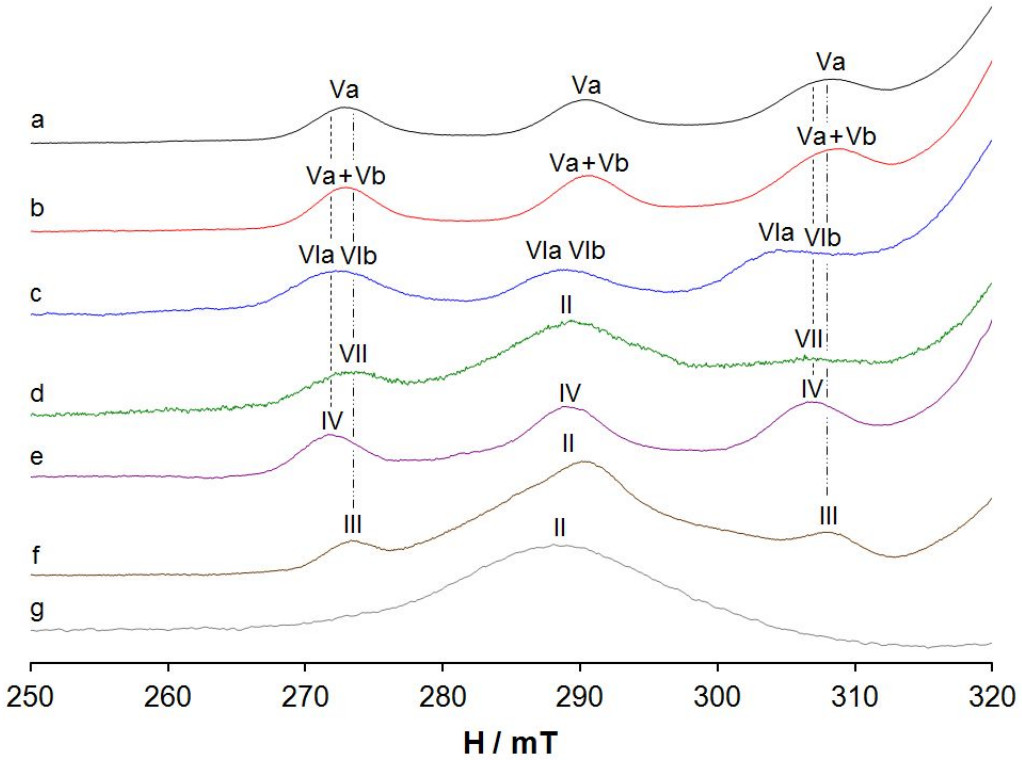

Figure 6 Low field region of the anisotropic X-band EPR spectra recorded at pH 7.4 on frozen solutions (120 K) containing: a) $^{63}Cu^{II}$/Me_2phen/Mb 1/1/1; b) $^{63}Cu^{II}$/Me_2phen/Mb 2/2/1; c) $^{63}Cu^{II}$/Me_2phen/Ub 1/1/1; d) $^{63}Cu^{II}$/Me_2phen/Lyz 1/1/1; e) $^{63}Cu^{II}$/Me_2phen/MeIm 1/1/1; f) $^{63}Cu^{II}$/Me_2phen/Gly 1/1/1; g) $^{63}Cu^{II}$/Me_2phen 1/1. In all the systems, the concentrations of $^{63}Cu^{II}$ and MOPS were 1.0×10^{-3} M and 0.1 M, respectively. **II**, **III**, **IV**, **Va**, **Vb**, **VIa**, **VIb**, and **VII** denote the resonances of the species $[Cu^{II}_2(Me_2phen)_2(OH)_2(H_2O)_2]^{2+}$, $[Cu^{II}(Me_2phen)(Gly)]^{+}$, $[Cu^{II}(Me_2phen)(MeIm)(H_2O)]^{2+}$, and of the adducts Mb–$[Cu^{II}(Me_2phen)]^{a}$, Mb–$[Cu^{II}(Me_2phen)]^{b}$, Ub–$[Cu^{II}(Me_2phen)]^{a}$, Ub–$[Cu^{II}(Me_2phen)]^{b}$, and Lyz–$[Cu^{II}(Me_2phen)]$, respectively. With the dotted and dot-dash-dot lines the first and third parallel resonances of $[Cu^{II}(Me_2phen)(MeIm)(H_2O)]^{2+}$ and $[Cu^{II}(Me_2phen)(Gly)]^{+}$, respectively, are indicated.

Docking calculations allowed us to identify two major binding sites of Mb capable of interacting with the $Cu^{II}(Me_2phen)^{2+}$ fragment by the simultaneous coordination of two residues and, therefore, with rather high thermodynamic stability: the first with one His and one carboxylate group (site 1 in Table 3 and Fig. 7a) and another with two histidine residues bound to the metal (site 2 in Table 3 and Fig. 7a). Four minor sites with intermediate or weak strength could involve the coordination of only one side-chain of a carboxylate group from Asp/Glu residues (site 3 in Table 3) or of a histidine residue (sites 4-5 in Table 3), all with a water ligand completing the equatorial donor set.

Site 1 involves the coordination of His81 and Glu83 (Fig. 7a); for site 2, the equatorial positions are occupied by His113 and His116 (Fig. 7b). Some examples for sites 3-5 with monodentate coordination of one Asp or one His are shown in Fig. S5 of ESI†. All the sites found by dockings are listed in Table 3, where the Cu–donor distances and GoldScore Fitness *F* values are also reported. The predicted bond lengths for the adducts are close to those predicted for Cu–N(imidazole) and Cu–O(carboxylate). Based on the maximum and mean Fitness (F_{max} and F_{mean}), the affinity order at physiological pH is: site 1 ~ site 2 >> sites 3-5, which suggests that sites 1 and 2 are populated before 3-5. Site 3 consists in turn of two poses, denoted by 3' and 3", with different donor atoms, namely Asp122 and Asp20, respectively. They can be considered as one only site, site 3, and not two separated sites, because they cannot be occupied simultaneously, Asp122 and Asp20 being too close in the tertiary structure of the protein. Thus, they are not independent from each other, but they have been considered as two possibilities for the same binding site. A similar case was encountered for site 1 of Ub (see below).

Therefore, the docking results confirm the ESI-MS and EPR data which show that at least two adducts with different donor set are formed in solution, those indicated with Mb–$[Cu^{II}(Me_2phen)]^{\mathbf{a}}$ and Mb–$[Cu^{II}(Me_2phen)]^{\mathbf{b}}$. On the basis of the calculations, one can imagine that the first $Cu^{II}(Me_2phen)^{2+}$ fragment binds to the couple (His81, Glu83) to form Mb–$[Cu^{II}(Me_2phen)]^{\mathbf{a}}$ (**Va** in Figs. 5 and 6), and the second one to the site (His113, His116) to give Mb–$[Cu^{II}(Me_2phen)]^{\mathbf{b}}$ (**Va** in Figs. 5 and 6). The possibility that, at lower protein/metal molar ratios, $Cu^{II}(Me_2phen)(H_2O)^{2+}$ binds to one His or Asp/Glu side-chain donor, suggested by dockings, cannot be excluded and their possible signals could contribute to the large resonances observed when $^{63}Cu^{II}$/Me_2phen/Mb ratio is 4/4/1 (trace c of Fig. 5).

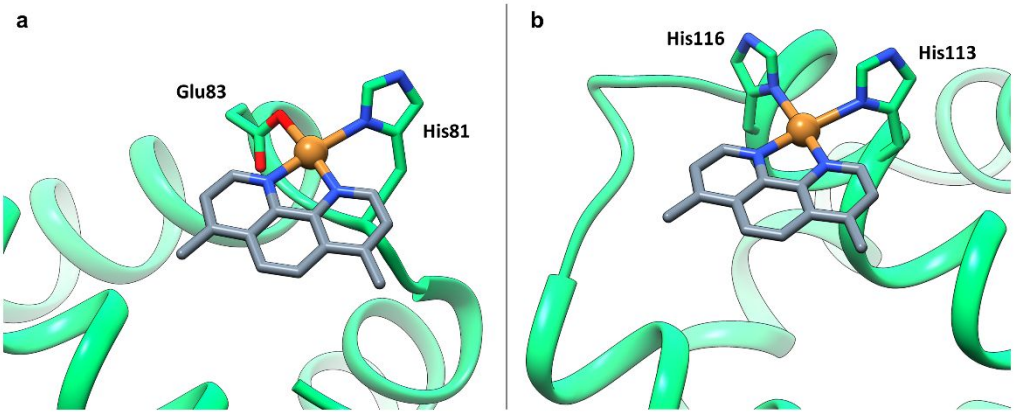

Fig. 7 Binding sites of holo-Mb for the fragment $Cu^{II}(Me_2phen)^{2+}$ from docking results: a) site 1; b) site 2 (see Table 3).

Table 3 Binding sites of the fragments $Cu^{II}(Me_2phen)^{2+}$ to Mb, Ub and Lyz proteins.

Protein	Site	Donors	Cu–N [a]	Cu–O [a]	F_{max} [b]	F_{mean} [c]	Pop. [d]
Mb	1	N_{His81}, COO^-_{Glu83}	2.403	2.424	58.3	53.8	74%
Mb	2	N_{His113}, N_{His116}	2.432, 2.463	–	52.8	50.4	66%
Mb	3'	COO^-_{Asp122} [e]	–	2.360	44.1	40.8	18%
Mb	3"	COO^-_{Asp20} [e]	–	2.412	41.8	40.2	82%
Mb	4	N_{His36}	2.420	–	41.4	40.0	98%
Mb	5	N_{His24}	2.354	–	30.3	30.3	2%
Ub	1'	COO^-_{Glu51}, COO^-_{Asp52} [e]	–	2.403, 2.230	54.5	50.2	68%
Ub	1"	COO^-_{Glu24}, COO^-_{Asp52} [e]	–	2.312, 2.292	46.8	42.6	10%
Ub	2	COO^-_{Glu18}, COO^-_{Asp21}	–	2.324, 2.422	52.2	48.1	26%
Ub	3	N_{His68}	2.205	–	42.4	41.0	98%
Lyz	1	COO^-_{Asp87}, OH_{Thr89}	–	2.236, 2.270	51.5	50.3	100%
Lyz	2	COO^-_{Glu35}, CO_{Leu56}	–	2.106, 2.258	48.6	45.3	88%
Lyz	3	COO^-_{Asp101}	–	2.030	36.2	36.2	2%

[a] Distances in Å. [b] Fitness value for the most stable pose of each cluster. [c] Mean Fitness value of the GoldScore scoring function for each cluster. [d] Percent population of the cluster. [e] Sites not independent on each other.

The position of the possible binding sites on the protein surface, unveiled by dockings, is shown in Fig. 8a. As it can be observed, more than one metal moieties can bind to myoglobin simultaneously and this suggests that – depending on the concentration of the metal fragment – one protein can transport several Cu^{II} fragments in biological fluids toward the molecular targets in the organism.

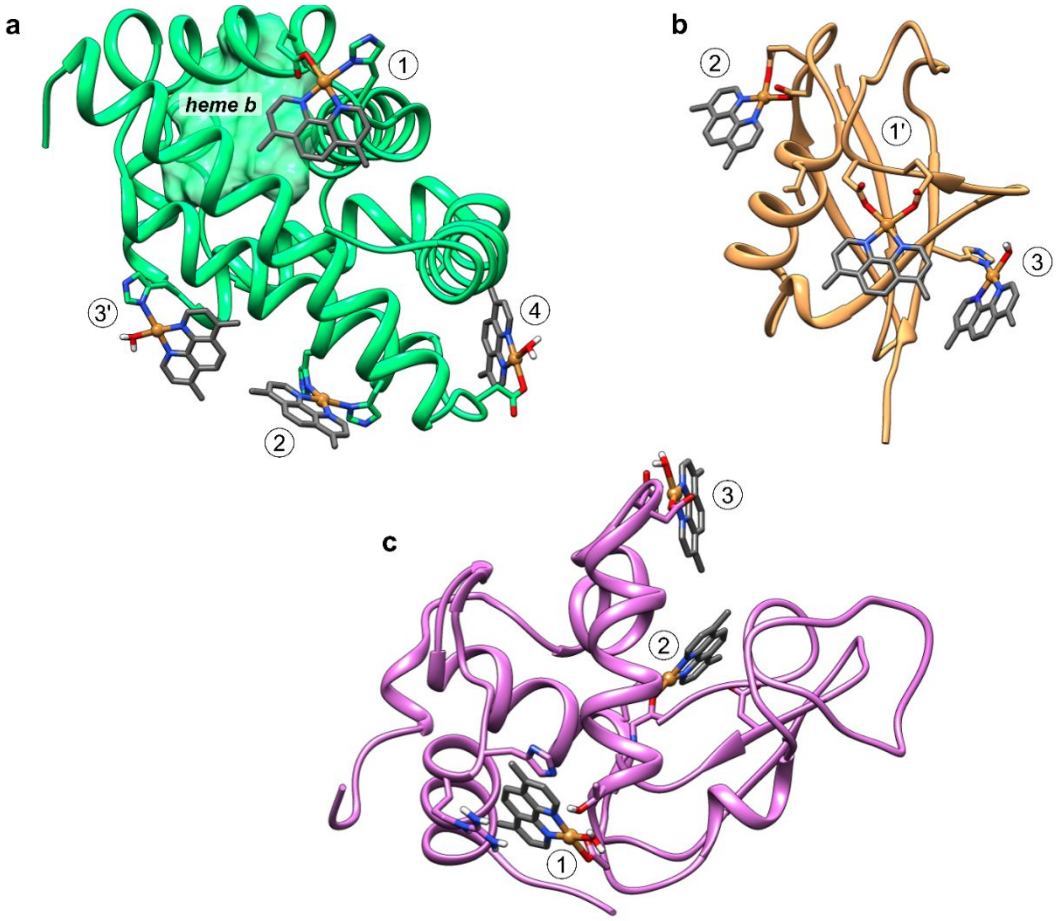

Fig. 8 Binding sites unveiled by docking simulations for $Cu^{II}(Me_2phen)^{2+}$ to the small proteins studies in this work: a) myoglobin (sites 1, 2, 3', and 4 are shown); b) ubiquitin (sites 1', 2, and 3); c) lysozyme (sites 1, 2, and 3). The heme b of myoglobin is indicated with the shaded green surface.

Systems Cu^{II}/Ub, Cu^{II}/Me_2phen/Ub and Cas II-gly/Ub

ESI-MS(+) spectra of free ubiquitin show the presence of several adducts with the ubiquitous ions Na^+ and K^+. The positive-ion mode spectra recorded in an aqueous solution give a pattern of peaks with different states of charges, having *z* ranging from +5 to +10, and corresponding to a mass of 8564.6 Da upon deconvolution, in agreement with previous papers in the literature.[31, 65]

The mass spectra of the system Cu^{II}/Me_2phen/Gly/Ub contain signals attributable to the adducts Ub–$[Cu^{II}(Me_2phen)]_n$ with n = 1-3, suggesting that the protein can bind more than one

$Cu^{II}(Me_2phen)^{2+}$ fragment at the same time and, therefore, that several binding sites exist. The deconvoluted mass spectrum in Fig. 9 consists of four sets of signals, each one composed of several peaks separated by the mass of a Na^+ ion. Even if in the deconvoluted spectrum the mass difference cannot be calculated unambiguously for the presence of many adducts with Na^+, the three sets of signals are separated from that of free protein by the masses corresponding to one, two, or three $Cu^{II}(Me_2phen)^{2+}$ fragments (*ca*. 271 Da).

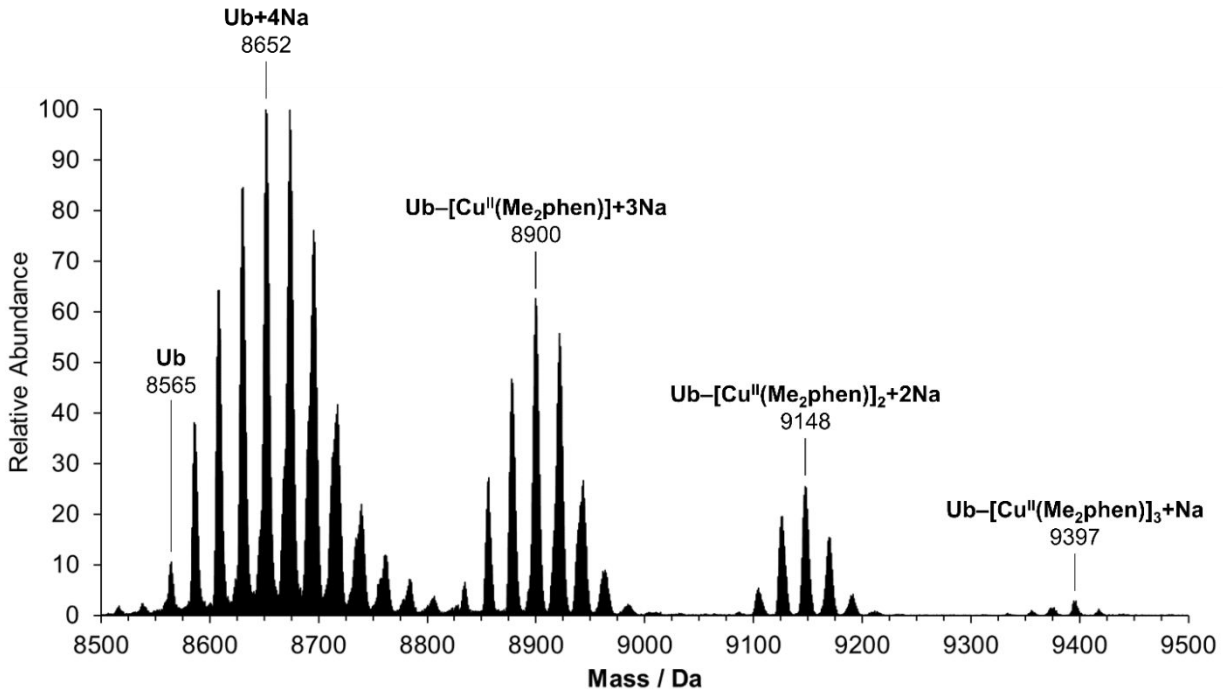

Fig. 9 Deconvoluted ESI-MS(+) spectrum of the system Cu^{II}/Me_2phen/Gly/Ub 5/5/5/1 in H_2O (MeOH 10%). The concentration of Ub 5 was μM.

For comparison, the ESI-MS(+) spectra of the system Cu^{II}/phen/Gly/Ub, i.e. that with Cas VII-gly, were also recorded and the deconvoluted signal showed two peaks at +241 and +485 Da compared to that of the free protein, attributable to the adducts Ub–[Cu^{II}(phen)], and Ub–[Cu^{II}(phen)]$_2$, the mass of the $Cu^{II}(phen)^{2+}$ moiety being *ca.* 244 Da (Fig. S6 of ESI†).

To unambiguously confirm the presence of these adducts in the systems with Me_2phen or phen, the simulations of selected peaks in the non-deconvoluted mass spectrum were carried out with Prot pi,[37] similarly to what has been described for Mb. The peaks of the free ubiquitin were simulated with the molecular formula $C_{378}H_{629}N_{105}O_{118}S$, which correspond to a mass of 8564.6 Da. The signals attributed to the adducts with one $Cu^{II}(Me_2phen)^{2+}$ (Fig. 10), two and three $Cu^{II}(Me_2phen)^{2+}$ (Figs. S7 and S8 of ESI†) were simulated for the peaks with z = +6, the most intense in the

spectrum.

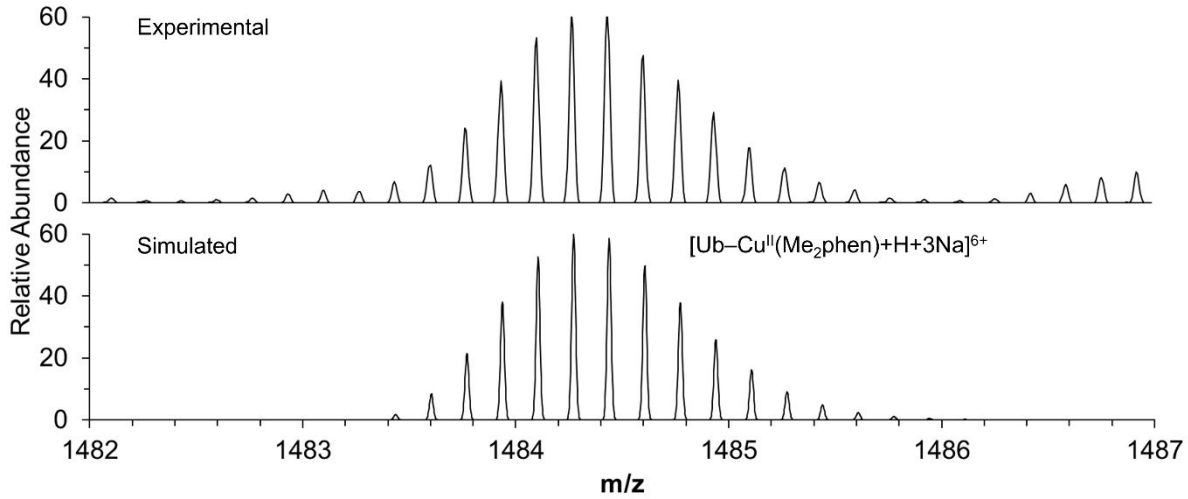

Fig. 10 ESI-MS(+) spectrum in the m/z range 1482-1487 of the system Cu^{II}/Me_2phen/Gly/Ub 5/5/5/1 in H_2O (MeOH 10%). The concentration of Ub was 5 μM. Comparison between the experimental (above) and the simulated (below) isotopic pattern for the molecular entity [Ub–Cu^{II}(Me_2phen)+H+3Na]$^{6+}$, where Ub stands for the neutral form of ubiquitin, with molecular formula $C_{378}H_{629}N_{105}O_{118}S$, and the formula of Cu^{II}(Me_2phen) is $C_{14}H_{12}Cu^{II}N_2^{2+}$. The abundance is relative to the signal of the free protein (not shown in this m/z range).

The signals of the adducts with one and two $Cu^{II}(phen)^{2+}$ were also simulated and compared with the experimental ones; the results are shown in Figs. S9 and S10 of ESI†, respectively. In all the examined cases (Fig. 10 and Figs. S7-S10 of ESI†), the agreement between the experimental observations and simulations confirms the attribution of the observed signals to Ub adducts with the fragment $Cu^{II}(Me_2phen)^{2+}$, deriving from Cas II-gly, and with the fragment $Cu^{II}(phen)^{2+}$, deriving from Cas VII-gly.

The EPR spectra recorded at LT on the system $^{63}Cu^{II}$/Me_2phen/Ub show a clear difference with that $^{63}Cu^{II}$/Me_2phen/Gly (cfr. traces c-e with trace a in Fig. 11). The signals are broad and suggest the presence of more than one adduct (resonances denoted with **VIa** and **VIb** in Fig. 11). The first, with g_z higher and A_z lower, is a species indicated with Ub–[Cu^{II}(Me_2phen)]$^{\mathbf{a}}$ (**VIa**), while the second one, with g_z lower and A_z larger can be identified with Ub–[Cu^{II}(Me_2phen)]$^{\mathbf{b}}$ (**VIb**). The spin Hamiltonian EPR parameters can be measured only approximately and are reported in Table 2. For Ub–[Cu^{II}(Me_2phen)]$^{\mathbf{b}}$, they are $g_z \sim 2.25$ and $A_z \sim 181 \times 10^{-4}$ cm^{-1} and are comparable to those of the mixed complex [Cu^{II}(Me_2phen)(MeIm)(H_2O)]$^{2+}$; therefore, they might be attributable to an

adduct with coordination mode (N_{phen}, N_{phen}); N_{His}; H_2O. In contrast, the parameters for Ub–[$Cu^{II}(Me_2phen)$][a], $g_z \sim 2.27$ and $A_z \sim 176 \times 10^{-4}$ cm^{-1}, are consistent with weaker donors, like one or two carboxylate groups occupying one or two equatorial positions. It is not possible to exclude that, below the large resonances, two different adducts with the same donor set, (N_{phen}, N_{phen}); ($COO^-_{Asp/Glu}$, $COO^-_{Asp/Glu}$), may exist. This would be in agreement with the ESI-MS measurements which show the presence of three adducts. The formation of adducts with ubiquitin based on the binding of various couples of carboxylate residues with ($COO^-_{Asp/Glu}$, $COO^-_{Asp/Glu}$) donor set was also demonstrated for pharmacologically active $V^{IV}O$ complexes.[31, 54c, 66]

The comparison with the behavior of the other systems with proteins shown in the trace c of Fig. 6 allows us to find further insights. The adducts with Ub (**VIa** and **VIb**) are formed by weaker donors with respect to those of myoglobin, discussed in the previous subsection, as shown by the higher g_z and lower A_z value. This is compatible with the binding of weak carboxylate groups in **VIa** and with the coordination of only one His residue in **VIb**. Therefore, EPR data indicate a different behavior of the two proteins; notably, the different binding modes, suggested by EPR spectroscopy, (N_{His}, $COO^-_{Asp/Glu}$) or (N_{His}, N_{His}) for Mb and ($COO^-_{Asp/Glu}$, $COO^-_{Asp/Glu}$) or (N_{His}) for Ub was confirmed by computational methods.

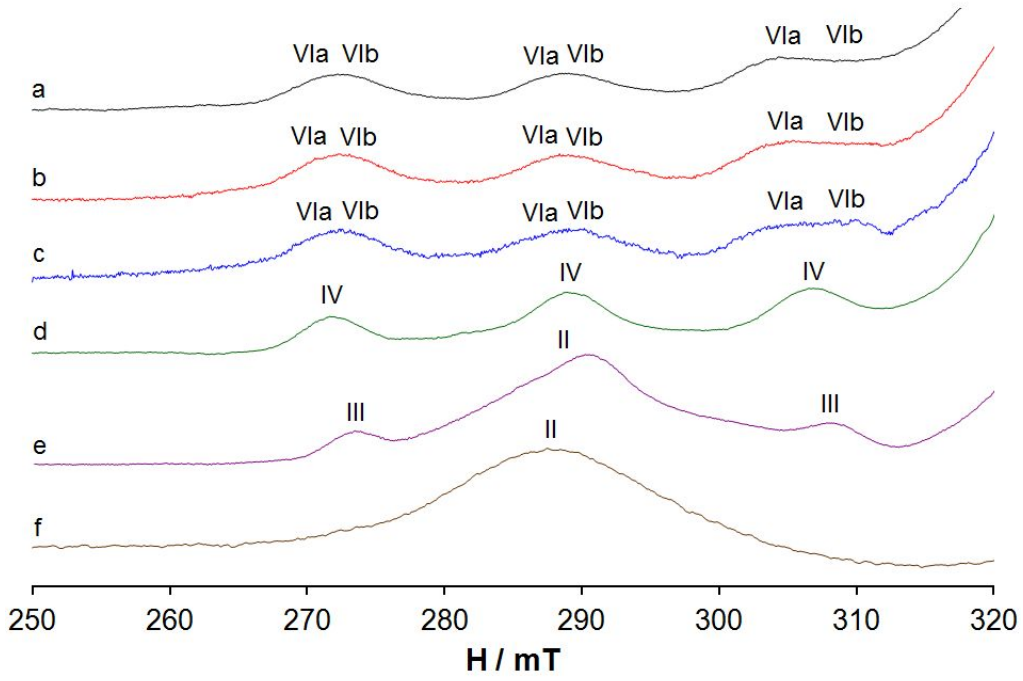

Fig. 11 Low-field region of anisotropic X-band EPR spectra recorded at pH 7.40 on frozen solutions (120 K) containing: a) $^{63}Cu^{II}$/Me_2phen/Ub 1/1/1; b) $^{63}Cu^{II}$/Me_2phen/Ub 2/2/1; c) $^{63}Cu^{II}$/Me_2phen/Ub 4/4/1; d) $^{63}Cu^{II}$/Me_2phen/MeIm 1/1/1; e) $^{63}Cu^{II}$/Me_2phen/Gly 1/1/1; f) $^{63}Cu^{II}$/Me_2phen 1/1. In all the systems, the concentrations of $^{63}Cu^{II}$ and MOPS were 1.0×10^{-3} M

and 0.1 M, respectively. **II**, **III**, **IV**, **VIa** and **VIb** denote the resonances of the species $[Cu^{II}_2(Me_2phen)_2(OH)_2(H_2O)_2]^{2+}$, $[Cu^{II}(Me_2phen)(Gly)]^{+}$, $[Cu^{II}(Me_2phen)(MeIm)(H_2O)]^{2+}$ and of the two adducts Ub–$[Cu^{II}(Me_2phen)]^{\mathbf{a}}$ and Ub–$[Cu^{II}(Me_2phen)]^{\mathbf{b}}$.

The docking results for ubiquitin suggest the presence of three binding sites for the fragment $Cu^{II}(Me_2phen)^{2+}$ (Fig. 12 and Table 3). One site (site 1 in Fig. 12a) is based on the simultaneous coordination of the side-chains of Asp or Glu residues and can be further divided in two 'subsites', denoted with 1' and 1' and involving Glu51 with Asp52 or Glu24 with Asp52, respectively. The simultaneous binding of two $Cu^{II}(Me_2phen)^{2+}$ moieties to such sites is not compatible; in other words, the sites 1' and 1" are not independent, similarly to the case of site 3 for Mb (*vide supra*). The second site (site 2, Fig. 12b) consists of two carboxylate donors from Glu18 and Asp21 and, for this reason, should have a strength similar to the sites1' and 1" and should not be distinguishable from them by EPR technique. As mentioned above, the sites 1 and 2 were also found for vanadium-based drugs,[31, 54c, 66] and could be equivalently populated having a comparable strength. The third (site 3, Fig. 12c) involves the mono-coordination of His68, the only histidine residue of protein, with the fourth equatorial position being occupied by a water molecule.

The presence of the sites 1, 2 and 3 accounts for ESI-MS and EPR data, which suggest the formation of two-three adducts, the first one with the $Cu^{II}(Me_2phen)^{2+}$ fragment bound to site 1 with bidentate coordination ($COO^{-}_{Glu/Asp}$, $COO^{-}_{Glu/Asp}$), the second bound to site 2 with the same donor set, and – finally – the third one $Cu^{II}(Me_2phen)^{2+}$ fragment bound to the site 3 with N_{His} monodentate binding. Moreover, the spectroscopic and computational data indicate that the ability of Cu^{II} to form coordinative bonds with ubiquitin is lower than with myoglobin, according to what was found for V^{IV} species.[27, 31] This could be due to the smaller dimension and number of potential strong donors of Ub in comparison with Mb (Table S2 of ESI†) and should be also considered that only one histidine residue (His68) – not too exposed on the surface – is present in its structure; in contrast Mb has eleven His residues, at least four of which available for metal coordination (His81, His113, His116, His119).[27] However, even though ubiquitin is a very small proteins with only 76 amino acids in comparison with 153 residues of myoglobin, it can bind at least three independent metal fragments in the sites 1, 2, and 3, their structure and position, found by docking calculations, being represented in Figs. 8 and 12.

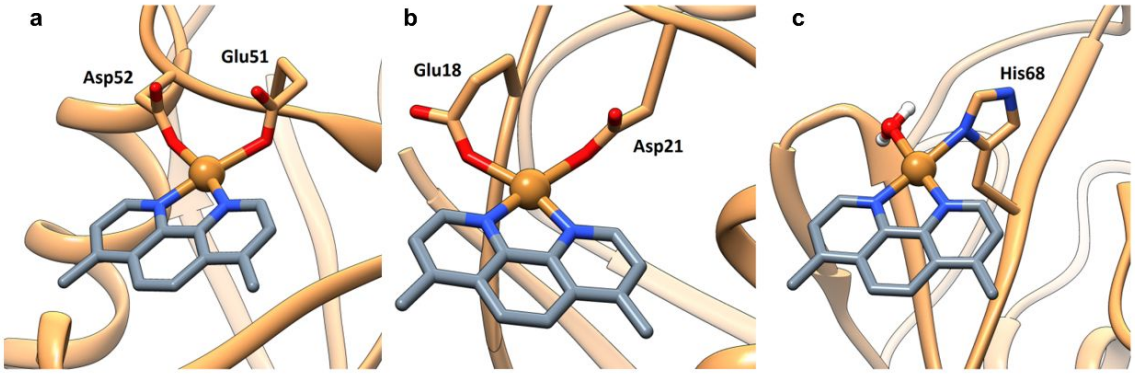

Fig. 12 Binding sites of Ub for the fragment $Cu^{II}(Me_2phen)^{2+}$ from docking results: a) site 1'; b) site 2; c) site 3 (see Table 3).

Systems $Cu^{II}/Me_2phen/Lyz$ and Cas II-gly/Lyz

ESI-MS(+) spectra of lysozyme in water exhibit resolved peaks with *z* between +7 and +12 in the *m*/*z* range 1100-2100, which agrees well with the literature data.[67, 68] These spectra were compared with those recorded on the systems with Cas II-gly. The deconvoluted spectrum of the system $Cu^{II}/Me_2phen/Gly/Lyz$ shows one peak at +270 Da compared to the peak of the pure protein (14305 Da) that can be attributed to the adduct Lyz–$[Cu^{II}(Me_2phen)]$ (Fig. 13). This attribution can be confirmed on the basis of the perfect agreement obtained simulating the ESI-MS(+) spectrum (Fig. 14, see below).

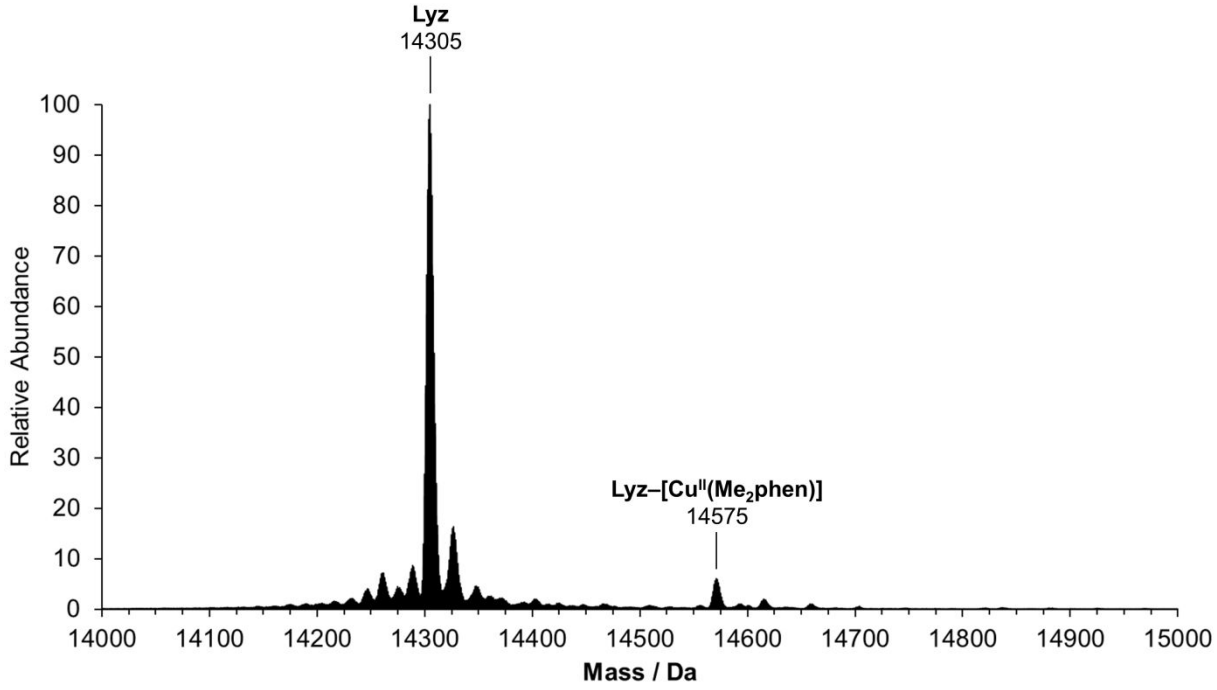

Fig. 13 Deconvoluted ESI-MS(+) of the system $Cu^{II}/Me_2phen/Gly/Lyz$ 3/3/3/1 in H_2O (MeOH

10%). The concentration of Lyz was 0.5 μM.

As done with ubiquitin, the existence of the adduct with lysozyme was substantiated by comparing the experimental and simulated ESI-MS(+) spectrum. In Fig. 14a, the experimental and simulated isotopic pattern for the peaks corresponding to the free protein at z = +10 (the most intense one) are presented, while in Fig. 14b the series of peaks of the molecular entity $[Lyz–Cu^{II}(Me_2phen)+8H]^{10+}$ (corresponding to the adduct $Lyz–[Cu^{II}(Me_2phen)]$) was successfully simulated. In particular, the peaks of the region with z = +10 account for the presence of free protein and of the adduct $Lyz–[Cu^{II}(Me_2phen)]$. The good agreement between the experimental and simulated patterns confirms that the signals in the ESI-MS(+) spectrum (Fig. 14), and in its deconvoluted form (Fig. 13), can be correctly attributed to the $Lyz–[Cu^{II}(Me_2phen)]$ adduct.

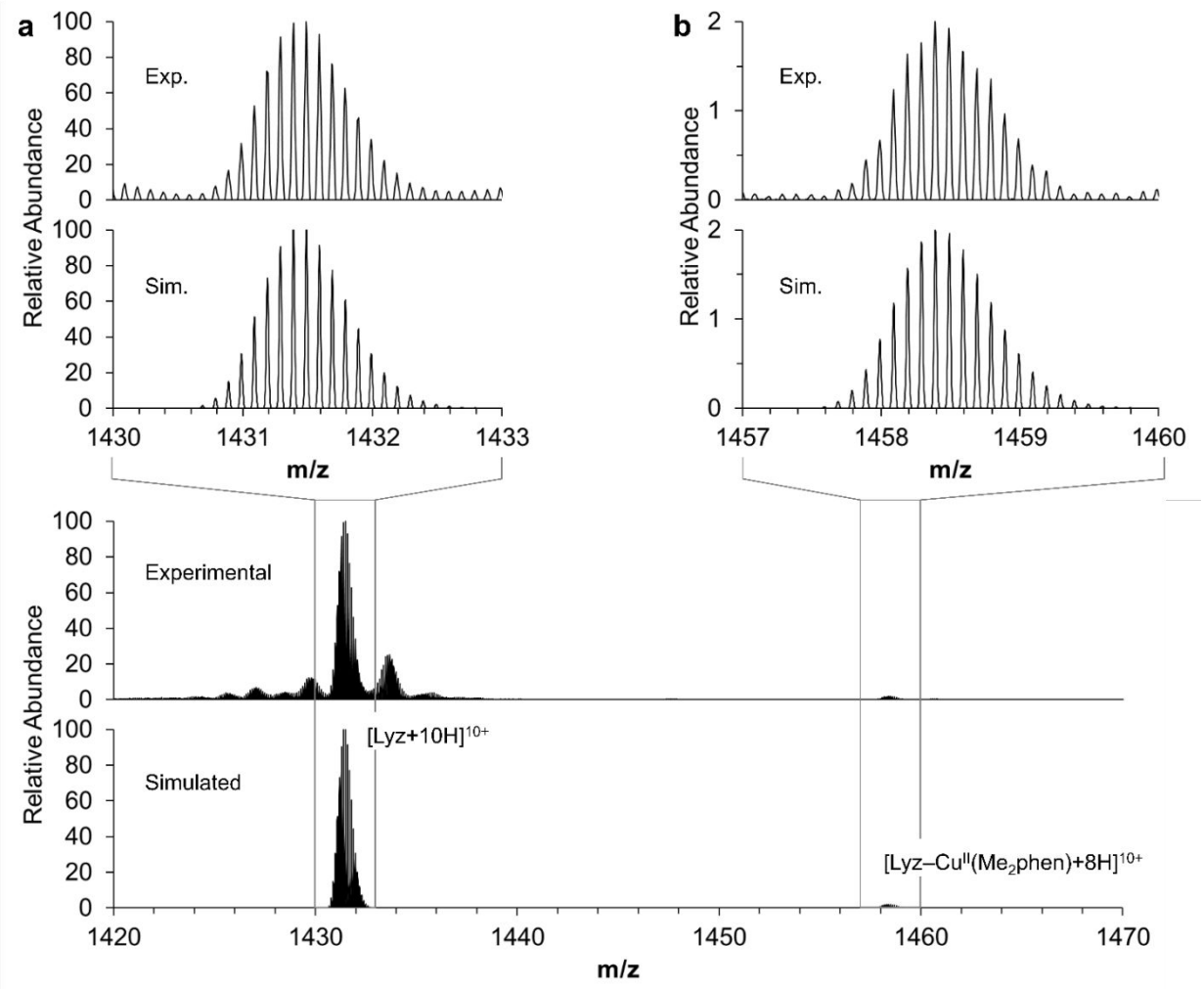

Fig. 14 Experimental and simulated ESI-MS(+) spectrum in the m/z range 1420-1470 of the system Cu^{II}/Me_2phen/Gly/Lyz 3/3/3/1, in H_2O (MeOH 10%). The concentration of Lyz was 5 μM.

In the lower part the comparison of the full region is presented. In the upper part the comparison is focused on the m/z = 1430-1433 region (signals of $[Lyz+10H]^{10+}$, letter a) and on the m/z = 1457-1460 region (signals of $[Lyz–Cu^{II}(Me_2phen)+8H]^{10+}$, letter b). In all the simulations, Lyz stands for the neutral form of lysozyme, with molecular formula $C_{613}H_{951}N_{193}O_{185}S_{10}$, while the formula of $Cu^{II}(Me_2phen)$ is $C_{14}H_{12}Cu^{II}N_2^{2+}$.

The EPR spectra of the system $Cu^{II}/Me_2phen/Lyz$ at LT are shown in Fig. 15. The spectrum obtained on the system Cu^{II}/Me_2phen, where only the broad signal of $[Cu^{II}_2(Me_2phen)_2(OH)_2(H_2O)_2]^{2+}$ appears, is reported as reference in the trace f (resonance indicated with **II**). In the spectra recorded with proteins, instead, beside the absorptions of $[Cu^{II}_2(Me_2phen)_2(OH)_2(H_2O)_2]^{2+}$, the signals of mononuclear adducts with lysozyme were detected (**VII** in the traces a-c of Fig. 15). This is in agreement with the ESI-MS measurements and demonstrates again that a protein with available side-chain donors partly suppresses hydrolysis and favors the formation of metal adducts. However, the presence of the resonances of hydrolyzed species $[Cu^{II}_2(Me_2phen)_2(OH)_2(H_2O)_2]^{2+}$ (**II**), which coexists with the adduct Lyz–$[Cu^{II}(Me_2phen)]$ (**VII**), suggests that the interaction with Lyz is weaker than in the systems containing myoglobin and ubiquitin, where the hydrolytic species is completely transformed in the adducts Ub/Mb–$[Cu^{II}(Me_2phen)]$. This is confirmed by an examination of Fig. 6 where it is evident that the relative intensity of the absorptions of Lyz–$[Cu^{II}(Me_2phen)]$ is much lower compared to that of the adducts formed with Mb and Ub (cfr. trace d with traces a-c of Fig. 6).

A comparison with the spectrum recorded with 1-methylimidazole (**IV** in the trace d of Fig. 15) shows that the hyperfine coupling constant of the adduct Lyz–$[Cu^{II}(Me_2phen)]$ is smaller than $[Cu^{II}(Me_2phen)(MeIm)(H_2O)]^{2+}$, suggesting that the donor(s) is(are) weaker, possibly provided with O atoms. The spin Hamiltonian parameters for this species (indicated with **VII**) are measurable only in an approximate way ($g_z \sim 2.25$ and $A_z \sim 174 \times 10^{-4}$ cm^{-1}, Table 2), suggesting that O donors from available amino acid side-chains could be bound to the $Cu^{II}(Me_2phen)^{2+}$ fragment. It must be noticed that, under the broad signals indicated by **VII**, the existence of more than one adduct with slightly different coordination modes cannot be excluded, as suggested by dockings (see below).

The comparison with the spectra of the adducts formed by myoglobin and ubiquitin is shown in Fig. 6: it can be observed that the resonance of the adduct formed by Lyz fall in a magnetic field range similar to that of the adducts of Ub, confirming that in both cases O donors bind Cu^{II} ion.

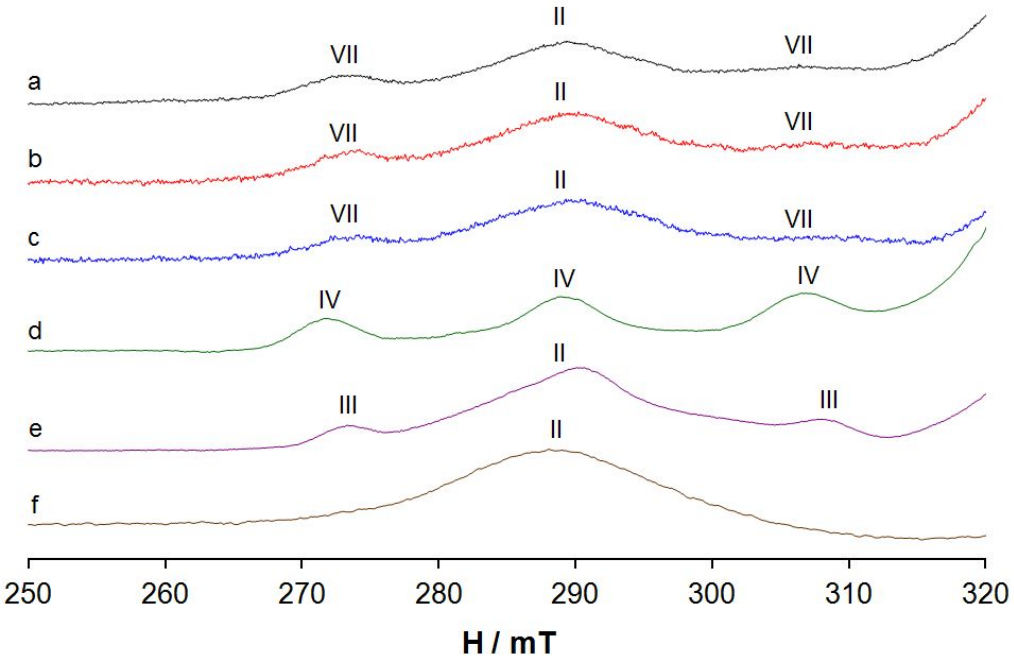

Fig. 15 Low-field region of anisotropic X-band EPR spectra recorded at pH 7.40 on frozen solutions (120 K) containing: a) $^{63}Cu^{II}$/Me_2phen/Lyz 1/1/1; b) $^{63}Cu^{II}$/Me_2phen/Lyz 2/2/1; c) $^{63}Cu^{II}$/Me_2phen/Lyz 4/4/1; d) $^{63}Cu^{II}$/Me_2phen/MeIm 1/1/1; e) $^{63}Cu^{II}$/Me_2phen/Gly 1/1/1; f) $^{63}Cu^{II}$/Me_2phen 1/1. In all the systems, the concentrations of $^{63}Cu^{II}$ and MOPS were 1.0×10^{-3} M and 0.1 M, respectively. **II**, **III**, **IV**, and **VII** denote the resonances of the species $[Cu^{II}_2(Me_2phen)_2(OH)_2(H_2O)_2]^{2+}$, $[Cu^{II}(Me_2phen)(Gly)]^+$, $[Cu^{II}(Me_2phen)(MeIm)(H_2O)]^{2+}$ and of the adduct Lyz–$[Cu^{II}(Me_2phen)]$.

The docking simulations show that at least three binding sites for the $Cu^{II}(Me_2phen)^{2+}$ moiety are possible (Fig. 16 and Table 3): the first site is bidentate, with the equatorial binding of Asp87 and the axial of OH group of Thr89 (site 1 in Fig. 16 and Table 3); notably, the carboxylate group of Asp87 was found to covalently interact with $[V^{IV}O(H_2O)_4]^{2+}$ [69] and with polyoxidovanadates $[V_{20}O_{54}(NO_3)]^{n-}$,[70, 71] and $[V_{20}O_{51}(OH_2)]^{n-}$,[71-72] with Thr89 residue stabilizing these adducts through H-bonds. The binding of $Cu^{II}(Me_2phen)^{2+}$ to the site 1 of lysozyme is stabilized by favorable van der Waals interaction with Arg 14 and His 15 residues; from an examination of Fig. 16a, the π–π contacts between Me_2phen ligand and the imidazole ring of His15 are well evident. The second site (site 2 in Fig. 16 and Table 3) is again bidentate and is based on carboxylate of Glu35 and carbonyl oxygen of Leu56. Finally, the third possible site (site 3 in Fig. 16 and Table 3) is monodentate with the coordination of Asp101, stabilized by the interaction with Asn103 residue through van der Waals forces (Fig. 16c).

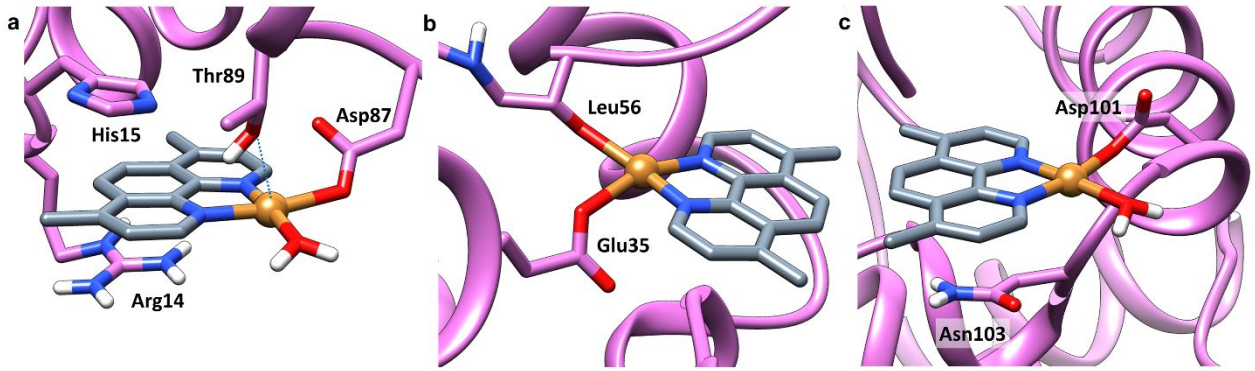

Fig. 16 Binding sites of Lyz for the fragment $Cu^{II}(Me_2phen)^{2+}$ from docking results: a) site 1; b) site 2; c) site 3 (see Table 3).

Therefore, the results of the dockings and the determination of the possible sites 1-3 confirm the possibility for the fragment $Cu^{II}(Me_2phen)^{2+}$ to bind with lysozyme. From the results, it appears that sites 1 and 2 are much stronger than site 3 but it is not clear with which of the two the moieties $Cu^{II}(Me_2phen)^{2+}$ interacts or if, instead, it is distributed on both of them, as could suggest the broad absorptions detected by EPR spectroscopy (see the resonances indicated by **VII** in the traces a-c of Fig. 15). However, the number of potential sites is lower than the ones of myoglobin despite the similar sizes of the two proteins (Table S2 of ESI†), and only O – and not N donors – should interact with the Cu^{II} center. Instead, the comparison with ubiquitin (Table S2 of ESI†) shows that the number of lysozyme sites is similar, with the majority of O donors. These should be preferred respect to the unique – and not sufficiently exposed on the protein surface – His residue in their structure (His68 for Ub and His15 for Lyz, Table S2 of ESI†); this is line with what was observed by EPR spectroscopy which shows a comparable behavior of Ub and Lyz. However, from an examination of the *F* values (Table 3), the binding of the $Cu^{II}(Me_2phen)^{2+}$ fragment to Lyz appears to be weaker than to Ub. Indeed, while for Ub there are at least two sites with the simultaneous binding of two carboxylate groups, in Lyz the only possible sites with a bidentate coordination (sites 1 and 2, Table 3) consist of one carboxylate plus a weaker O donor, such as OH of Thr and CO of Leu. Moreover, the dockings allowed us to exclude the binding of His15, not accessible for the $Cu^{II}(Me_2phen)^{2+}$ moiety. This allows rationalizing the behavior observed with ESI-MS and EPR techniques.

Conclusions

Casiopeínas® are a family of patented anticancer Cu^{II} compounds, but their action mechanism in the organism is not known and remains to be completely elucidated. Particularly, the transport in biological fluids and the form in which they reach the targets in the organism represent a relevant issue related to their pharmacological activity. In fact, in solution, Cas II-gly and Cas VII-gly can keep their identity or give several reactions: the replacement of glycinato or Me_2phen/phen or both of them by bioligands to form mixed or binary species with formula Cu^{II}–Me_2phen–bioligand, Cu^{II}–Gly–bioligand, or Cu^{II}–bioligand. Among the bioligands, proteins constitute a special class because of the high affinity toward the metal ions for the large number of binding sites and possible stabilization through secondary forces; consequently, adducts with composition Protein–$[Cu^{II}(Me_2phen)(Gly)]_n$, Protein–$[Cu^{II}(Me_2phen)]_n$, Protein–$[Cu^{II}(Gly)]_n$, or Protein–$[Cu^{II}]_n$, with a variable value of *n*, could be formed. These adducts may deactivate the administrated compound or, conversely, facilitate the uptake by target cells. Therefore, it is essential to know the reaction of Casiopeínas® in the presence of proteins to identify the active species in the organism.

For this series of reasons, the transport and action mode of Casiopeínas® remain interesting challenges for bioinorganic and medicinal chemistry and in this work we decided to continue the research started with the examination of their speciation with lmm bioligands through a multistep project.[17] In particular, we presented the interaction of Casiopeínas® with model proteins at 25 °C, while two additional studies are in progress on their binding to the most important serum proteins, HTf and HSA, at 25 °C and on the behavior of Casiopeínas® in plasma samples, i.e., in systems containing both blood proteins and lmm bioligands at 37 °C employing the same experimental approach used for pharmacologically active vanadium compounds.[73] Here, we demonstrated that, in the presence of small proteins such as myoglobin (Mb), ubiquitin (Ub) and lysozyme (Lyz), adducts with formula Protein–$[Cu^{II}(Me_2phen)]_n$ with n = 1, 2, or 3 are formed after the replacement of glycinato in the equatorial positions. It is interesting to observe that, depending on the protein, the binding mode can be mono- or bidentate and that the used donor set can be (N_{His}, N_{His}), (N_{His}, $COO^-_{Asp/Glu}$), ($COO^-_{Glu/Asp}$, $COO^-_{Glu/Asp}$), ($COO^-_{Glu/Asp}$, CO) or only monodentate His-N or O donors. Moreover, each protein is provided with several sites and can bind at least three metal fragments simultaneously. Therefore, it is expected that proteins like transferrin or albumin in blood serum, hemoglobin in the erythrocytes and cellular proteins could give adducts like Protein–$[Cu^{II}(Me_2phen)]_n$, with n larger than 2-3, using different amino acid couples; the adducts could be stabilized by H-bonds or other secondary van der Waals interactions.

The formed adducts are rather stable, as it can be ascertained by mass spectrometry and EPR spectroscopy results, even if the determination of the association constants is beyond the scopes of this work. At the moment, it is unclear whether the formation of the adducts leads to a beneficial

effect or not regarding activity of Casiopeínas®; in fact, if one hand the interaction can facilitate the transport in blood and the uptake into the cells (for example, in the case of adducts with holo-HTf that could be internalized through endocytosis), on the other the formation of stable adducts could deactivate the metal-drugs. It cannot be excluded that, at the metal concentrations found in the organism after the administration of a metal drug, the adducts Protein–$[Cu^{II}(Me_2phen)]_n$ coexist with $[Cu^{II}(Me_2phen)(Gly)]^+$ and other mixed species with formula Cu^{II}–Me_2phen–bioligand, where bioligands may be – as demonstrated recently [17] – small molecules of blood serum (citrate, lactate, and histidine) and cytosol (GSH, NADH, ATP, and L-ascorbate). The (final) destiny of the fragment $Cu^{II}(Me_2phen)^{2+}$ inside the cells is not clear. Costa Pessoa and coworkers have recently shown that in the systems Cu^{II}/phen the interaction with the cellular components and the consequent cell death is attributable to the separate actions of Cu^{2+} ions on one hand and free phenanthroline ligand on the other hand.[74] Certainly, at low metal concentrations found in cells, the tendency for dissociation of $Cu^{II}(Me_2phen)^{2+}$ is favoured but this might be only partial and a mixture of species could be responsible of the biological effects of Casiopeínas®. Therefore, the major challenge in this field is determining if, at cellular copper concentrations, the adducts with proteins are completely dissociated or if, in contrast, maintain partly their identity. The results of this work – even if not conclusive – can lay the basis for subsequent studies to understand which of the two alternatives, or both together, is the correct one.

Data availability statement

The data supporting this article have been included as part of the Electronic Supplementary Information.

Conflicts of interest

There are no conflicts to declare.

Acknowledgements

E.G. thanks MIUR PRIN 2022 - project cod. 2022APCTNA "*TRILLI – TRansforming metal Ions and Low-cost LIgands into next generation metallodrugs. A thermodynamic, spectroscopic and biological approach for their rational design*" for supporting this research. G.S. thanks Ministerio de Ciencia e Innovación for Grant PID2023-149492NB-I00.

5. References

1. *World Health Organization, https://www.who.int (last accessed 10 March 2025)*.
2. (a) K. D. Mjos and C. Orvig, Metallodrugs in Medicinal Inorganic Chemistry, *Chem. Rev.*, 2014, **114**, 4540-4563; (b) E. J. Anthony, E. M. Bolitho, H. E. Bridgewater, O. W. L. Carter, J. M. Donnelly, C. Imberti, E. C. Lant, F. Lermyte, R. J. Needham, M. Palau, P. J. Sadler, H. Shi, F.-X. Wang, W.-Y. Zhang and Z. Zhang, Metallodrugs are unique: opportunities and challenges of discovery and development, *Chem. Sci.*, 2020, **11**, 12888-12917; (c) I. Yousuf, M. Bashir, F. Arjmand and S. Tabassum, Advancement of metal compounds as therapeutic and diagnostic metallodrugs: Current frontiers and future perspectives, *Coord. Chem. Rev.*, 2021, **445**, 214104; (d) E. Fotopoulou, I. Titilas and L. Ronconi, Metallodrugs as Anticancer Chemotherapeutics and Diagnostic Agents: A Critical Patent Review (2010-2020), *Recent Pat. Anti-Cancer Drug Discovery*, 2022, **17**, 42-54; (e) V. M. Miranda, Medicinal inorganic chemistry: an updated review on the status of metallodrugs and prominent metallodrug candidates, *Rev. Inorg. Chem.*, 2022, **42**, 29-52.
3. (a) K. D. Karlin and Z. Tyeklár, *Bioinorganic Chemistry of Copper*, Chapman & Hall, Inc., New York, NY, 1993; (b) R. A. Festa and D. J. Thiele, Copper: An essential metal in biology, *Curr. Biol.*, 2011, **21**, R877-R883; (c) W. Maret and A. Wedd, *Binding, Transport and Storage of Metal Ions in Biological Cells*, The Royal Society of Chemistry, 2014; (d) D. Rehder, *Bioinorganic Chemistry*, Oxford University Press, Oxford, 2014.
4. (a) C. Marzano, M. Pellei, F. Tisato and C. Santini, Copper Complexes as Anticancer Agents, *Anti-Cancer Agents Med. Chem.*, 2009, **9**, 185-211; (b) A. Hussain, M. F. AlAjmi, M. T. Rehman, S. Amir, F. M. Husain, A. Alsalme, M. A. Siddiqui, A. A. AlKhedhairy and R. A. Khan, Copper(II) complexes as potential anticancer and Nonsteroidal anti-inflammatory agents: In vitro and in vivo studies, *Sci. Rep.*, 2019, **9**, 5237; (c) F. Tisato, C. Marzano, M. Porchia, M. Pellei and C. Santini, Copper in diseases and treatments, and copper-based anticancer strategies, *Med. Res. Rev.*, 2010, **30**, 708-749; (d) I. Iakovidis, I. Delimaris and S. M. Piperakis, Copper and Its Complexes in Medicine: A Biochemical Approach, *Mol. Biol. Int.*, 2011, 594529; (e) C. Santini, M. Pellei, V. Gandin, M. Porchia, F. Tisato and C. Marzano, Advances in Copper Complexes as Anticancer Agents, *Chem. Rev.*, 2014, **114**, 815-862; (f) A. Kellett, Z. Molphy, V. McKee and C. Slator, in *Metal-based Anticancer Agents*, eds. A. Casini, A. Vessières and S. M. Meier-Menches, The Royal Society of Chemistry, Croydon, United Kingdom, 2019, pp. 91-119.
5. A. Bergamo and G. Sava, Linking the future of anticancer metal-complexes to the therapy of

tumour metastases, *Chem. Soc. Rev.*, 2015, **44**, 8818-8835.

6. Q. Peña, G. Sciortino, J.-D. Maréchal, S. Bertaina, A. J. Simaan, J. Lorenzo, M. Capdevila, P. Bayón, O. Iranzo and Ò. Palacios, Copper(II) N,N,O-Chelating Complexes as Potential Anticancer Agents, *Inorg. Chem.*, 2021, **60**, 2939-2952.
7. (a) D. Denoyer, S. A. S. Clatworthy and M. A. Cater, in *Metallo-Drugs: Development and Action of Anticancer Agents*, eds. A. Sigel, H. Sigel, E. Freisinger and R. K. O. Sigel, De Gruyter, Berlin, 2018, pp. 469-506; (b) M. Mathuber, S. Hager, B. K. Keppler, P. Heffeter and C. R. Kowol, Liposomal formulations of anticancer copper(II) thiosemicarbazone complexes, *Dalton Trans.*, 2021, **50**, 16053-16066.
8. V. Kannappan, M. Ali, B. Small, G. Rajendran, S. Elzhenni, H. Taj, W. Wang and Q. P. Dou, Recent Advances in Repurposing Disulfiram and Disulfiram Derivatives as Copper-Dependent Anticancer Agents, *Front. Mol. Biosci.*, 2021, **8**, 741316.
9. S. Abdolmaleki, A. Aliabadi and S. Khaksar, Unveiling the promising anticancer effect of copper-based compounds: a comprehensive review, *J. Cancer Res. Clin. Oncol.*, 2024, **150**, 213.
10. J. B. W. Hilton, K. Kysenius, J. R. Liddell, S. W. Mercer, B. Paul, J. S. Beckman, C. A. McLean, A. R. White, P. S. Donnelly, A. I. Bush, D. J. Hare, B. R. Roberts and P. J. Crouch, Evidence for disrupted copper availability in human spinal cord supports CuII(atsm) as a treatment option for sporadic cases of ALS, *Scientific Reports*, 2024, **14**, 5929.
11. A. Natarajan, S. M. Srinivas, C. Azevedo, L. Greene, A.-L. Bauchet, E. Jouannot, A.-S. Lacoste-Bourgeacq, I. Guizon, P. Cohen, A.-L. Naneix, O. Ilovich, J. Cisneros, K. Rupanarayan, F. T. Chin, A. Iagaru, F. M. Dirbas, A. Karam and S. S. Gambhir, Two Patient Studies of a Companion Diagnostic Immuno-Positron Emission Tomography (PET) Tracer for Measuring Human CA6 Expression in Cancer for Antibody Drug Conjugate (ADC) Therapy, *Mol. Imaging*, 2020, **19**, 1536012120939398.
12. C. Rivera-Guevara, M. E. Bravo-Gómez and L. Ruiz-Azuara, in *Molecular Oncology: Principles and Recent Advances*, ed. J. Camacho, Bentham, 2012, pp. 172-191.
13. (a) L. Ruiz-Azuara, Preparation of new mixed copper aminoacidate complexes from phenylate phenathrolines to be used as “anticancerigenic" agents, 07/628,628: Re 635,458. 1992, USA; (b) L. Ruiz-Azuara, Process to obtain new mixed copper aminoacidate complexes from phenylatephenanthroline to be used as anticancerigenic agents, 07/628,843: RE 635,458, Feb. 618 (1997). 1992, United States Patent; (c) L. Ruiz-Azuara, Copper amino acidate diimine nitrate compounds and their methyl derivatives and a process for preparing them, 07/628,628: 625,576,326. 1996, United States Patent.

14. (a) Y. Figueroa-DePaz, K. Resendiz-Acevedo, S. G. Dávila-Manzanilla, J. C. García-Ramos, L. Ortiz-Frade, J. Serment-Guerrero and L. Ruiz-Azuara, DNA, a target of mixed chelate copper(II) compounds (Casiopeinas®) studied by electrophoresis, UV–vis and circular dichroism techniques, *J. Inorg. Biochem.*, 2022, **231**, 111772; (b) Y. Figueroa-DePaz, J. Pérez-Villanueva, O. Soria-Arteche, D. Martínez-Otero, V. Gómez-Vidales, L. Ortiz-Frade and L. Ruiz-Azuara, Casiopeinas of Third Generations: Synthesis, Characterization, Cytotoxic Activity and Structure–Activity Relationships of Mixed Chelate Compounds with Bioactive Secondary Ligands, *Molecules*, 2022, **27**, 3504; (c) Z. Aguilar-Jiménez, A. Espinoza-Guillén, K. Resendiz-Acevedo, I. Fuentes-Noriega, C. Mejía and L. Ruiz-Azuara, The Importance of Being Casiopeina as Polypharmacologycal Profile (Mixed Chelate–Copper (II) Complexes and Their In Vitro and In Vivo Activities), *Inorganics*, 2023, **11**, 394.
15. (a) X. Solans, L. Ruiz-Ramirez, A. Martinez, L. Gasque and J. L. Brianso, Structures of chloro(glycinato)(1,10-phenanthroline)copper(II) monohydrate (I) and aqua(1,10-phenanthroline)(l-phenylalaninato)copper(II) nitrate monohydrate (II), *Acta Crystallogr., Sect. C: Cryst. Struct. Commun.*, 1988, **44**, 628-631; (b) X. Solans, L. Ruiz-Ramirez, A. Martinez, L. Gasque and R. Moreno-Esparza, Mixed chelate complexes. III. Structures of (l-alaninato)(aqua)(2,2'-bipyridine)copper(II) nitrate monohydrate and aqua(2,2'-bipyridine)(l-tyrosinato)copper(II) chloride trihydrate, *Acta Crystallogr., Sect. C: Cryst. Struct. Commun.*, 1992, **48**, 1785-1788; (c) X. Solans, L. Ruiz-Ramirez, A. Martinez, L. Gasque and R. Moreno-Esparza, Mixed chelate complexes. II. Structures of l-alaninato(aqua)(4,7-diphenyl-1,10-phenanthroline)copper(II) nitrite monohydrate and aqua(4,7-dimethyl-1,10-phenanthroline)(glycinato)(nitrato)copper(II) monohydrate, *Acta Crystallogr., Sect. C: Cryst. Struct. Commun.*, 1993, **49**, 890-893.
16. M. E. Bravo-Gómez, J. C. García-Ramos, I. Gracia-Mora and L. Ruiz-Azuara, Antiproliferative activity and QSAR study of copper(II) mixed chelate [Cu(N–N)(acetylacetonato)]NO_3 and [Cu(N–N)(glycinato)]NO_3 complexes, (Casiopeínas®), *J. Inorg. Biochem.*, 2009, **103**, 299-309.
17. V. Ugone, F. Pisanu, D. Sanna and E. Garribba, Interaction of the potent antitumoral compounds Casiopeinas® with blood serum and cellular bioligands, *J. Inorg. Biochem.*, 2021, **224**, 111566.
18. T. Kiss, É. A. Enyedy, T. Jakusch and O. Dömötör, Speciation of Metal Complexes of Medicinal Interest: Relationship between Solution Equilibria and Pharmaceutical Properties, *Curr. Med. Chem.*, 2019, **26**, 580-606.
19. R. Dinda, E. Garribba, D. Sanna, D. C. Crans and J. Costa Pessoa, Hydrolysis, Ligand

Exchange, and Redox Properties of Vanadium Compounds: Implications of Solution Transformation on Biological, Therapeutic, and Environmental Applications, *Chem. Rev.*, 2025, **125**, 1468-1603.

20. I. Correia, S. Borovic, I. Cavaco, C. P. Matos, S. Roy, H. M. Santos, L. Fernandes, J. L. Capelo, L. Ruiz-Azuara and J. Costs Pessoa, Evaluation of the binding of four anti-tumor Casiopeínas® to human serum albumin, *J. Inorg. Biochem.*, 2017, **175**, 284-297.
21. C. G. Hartinger, M. Groessl, S. M. Meier, A. Casini and P. J. Dyson, Application of mass spectrometric techniques to delineate the modes-of-action of anticancer metallodrugs, *Chem. Soc. Rev.*, 2013, **42**, 6186-6199.
22. M. Wenzel and A. Casini, Mass spectrometry as a powerful tool to study therapeutic metallodrugs speciation mechanisms: Current frontiers and perspectives, *Coord. Chem. Rev.*, 2017, **352**, 432-460.
23. A. Giorgio and A. Merlino, Gold metalation of proteins: Structural studies, *Coord. Chem. Rev.*, 2020, **407**, 213175.
24. D. Loreto and A. Merlino, The interaction of rhodium compounds with proteins: A structural overview, *Coord. Chem. Rev.*, 2021, **442**, 213999.
25. J. Schaller, S. Gerber, U. Kämpfer, S. Lejon and C. Trachsel, *Human Blood Plasma Proteins: Structure and Function*, John Wiley & Sons Ltd., Chichester, 2008.
26. (a) C. L. Behnes, J. Bedke, S. Schneider, S. Küffer, A. Strauss, F. Bremmer, P. Ströbel and H. J. Radzun, Myoglobin expression in renal cell carcinoma is regulated by hypoxia, *Exp. Mol. Pathol.*, 2013, **95**, 307-312; (b) S. Meller, A. Bicker, M. Montani, K. Ikenberg, B. Rostamzadeh, V. Sailer, P. Wild, D. Dietrich, B. Uhl, T. Sulser, H. Moch, T. A. Gorr, C. Stephan, K. Jung, T. Hankeln and G. Kristiansen, Myoglobin expression in prostate cancer is correlated to androgen receptor expression and markers of tumor hypoxia, *Virchows Arch.*, 2014, **465**, 419-427.
27. G. Sciortino, D. Sanna, V. Ugone, J. D. Marechal and E. Garribba, Integrated ESI-MS/EPR/computational characterization of the binding of metal species to proteins: vanadium drug-myoglobin application, *Inorg. Chem. Front.*, 2019, **6**, 1561-1578.
28. C. G. Hartinger, W. H. Ang, A. Casini, L. Messori, B. K. Keppler and P. J. Dyson, Mass spectrometric analysis of ubiquitin–platinum interactions of leading anticancer drugs: MALDI versus ESI, *J. Anal. At. Spectrom.*, 2007, **22**, 960-967.
29. (a) D. Gibson and C. Costello, A mass spectral study of the binding of the anticancer drug cisplatin to ubiquitin, *Eur. J. Mass Spectrom.*, 1999, **5**, 501-510; (b) J. P. Williams, H. I. A. Phillips, I. Campuzano and P. J. Sadler, Shape changes induced by N-terminal platination of

ubiquitin by cisplatin, *J. Am. Soc. Mass Spectrom.*, 2010, **21**, 1097-1106.

30. C. G. Hartinger, A. Casini, C. Duhot, Y. O. Tsybin, L. Messori and P. J. Dyson, Stability of an organometallic ruthenium-ubiquitin adduct in the presence of glutathione: relevance to antitumour activity, *J. Inorg. Biochem.*, 2008, **102**, 2136-2141.
31. V. Ugone, D. Sanna, G. Sciortino, J. D. Marechal and E. Garribba, Interaction of Vanadium(IV) Species with Ubiquitin: A Combined Instrumental and Computational Approach, *Inorg. Chem.*, 2019, **58**, 8064-8078.
32. S. A. Ragland and A. K. Criss, From bacterial killing to immune modulation: Recent insights into the functions of lysozyme, *PLoS Pathog.*, 2017, **13**, e1006512.
33. H. A. McKenzie and F. H. White, in *Adv. Protein Chem.*, eds. C. B. Anfinsen, F. M. Richards, J. T. Edsall and D. S. Eisenberg, Academic Press, 1991, pp. 173-315.
34. A. Merlino, Interactions between proteins and Ru compounds of medicinal interest: A structural perspective, *Coord. Chem. Rev.*, 2016, **326**, 111-134.
35. A. Merlino, Recent advances in protein metalation: structural studies, *Chem. Commun.*, 2021, **57**, 1295-1307.
36. M. T. Marty, A. J. Baldwin, E. G. Marklund, G. K. A. Hochberg, J. L. P. Benesch and C. V. Robinson, Bayesian Deconvolution of Mass and Ion Mobility Spectra: From Binary Interactions to Polydisperse Ensembles, *Anal. Chem.*, 2015, **87**, 4370-4376.
37. *Prot Pi, https://www.protpi.ch/ (last accessed 10 March 2025)*.
38. K. Chu, J. Vojtchovský, B. H. McMahon, R. M. Sweet, J. Berendzen and I. Schlichting, Structure of a ligand-binding intermediate in wild-type carbonmonoxy myoglobin, *Nature*, 2000, **403**, 921-923.
39. (a) F. He, C. L. Hendrickson and A. G. Marshall, Unequivocal determination of metal atom oxidation state in naked heme proteins: Fe(III)myoglobin, Fe(III)cytochrome c, Fe(III)cytochrome b5, and Fe(III)cytochrome b5 L47R, *J. Am. Soc. Mass Spectrom.*, 2000, **11**, 120-126; (b) Y. T. Li, Y. L. Hsieh, J. D. Henion and B. Ganem, Studies on heme binding in myoglobin, hemoglobin, and cytochrome c by ion spray mass spectrometry, *J. Am. Soc. Mass Spectrom.*, 1993, **4**, 631-637.
40. L. E. Sojo, N. Chahal and B. O. Keller, Oxidation of catechols during positive ion electrospray mass spectrometric analysis: Evidence for in-source oxidative dimerization, *Rapid Commun. Mass Spectrom.*, 2014, **28**, 2181-2190.
41. G. Prag, S. Misra, E. A. Jones, R. Ghirlando, B. A. Davies, B. F. Horazdovsky and J. H. Hurley, Mechanism of Ubiquitin Recognition by the CUE Domain of Vps9p, *Cell*, 2003, **113**, 609-620.

42. R. D. Palmiter, J. Gagnon, L. H. Ericsson and K. A. Walsh, Precursor of egg white lysozyme. Amino acid sequence of an NH_2-terminal extension, *J. Biol. Chem.*, 1977, **252**, 6386-6393.
43. M. J. Frisch, G. W. Trucks, H. B. Schlegel, G. E. Scuseria, M. A. Robb, J. R. Cheeseman, G. Scalmani, V. Barone, G. A. Petersson, H. Nakatsuji, M. Caricato, M. A. A., J. Bloino, B. G. Janesko, R. Gomperts, B. Mennucci, H. P. Hratchian, J. V. Ortiz, A. F. Izmaylov, J. L. Sonnenberg, D. Williams-Young, F. Ding, F. Lipparini, F. Egidi, J. Goings, B. Peng, A. Petrone, T. Henderson, D. Ranasinghe, V. G. Zakrzewski, J. Gao, N. Rega, G. Zheng, W. Liang, M. Hada, M. Ehara, K. Toyota, R. Fukuda, J. Hasegawa, M. Ishida, T. Nakajima, Y. Honda, O. Kitao, H. Nakai, T. Vreven, K. Throssell, J. A. Montgomery, Jr., J. E. Peralta, F. Ogliaro, M. J. Bearpark, J. J. Heyd, E. N. Brothers, K. N. Kudin, V. N. Staroverov, T. A. Keith, R. Kobayashi, J. Normand, K. Raghavachari, A. P. Rendell, J. C. Burant, S. S. Iyengar, J. Tomasi, M. Cossi, J. M. Millam, M. Klene, C. Adamo, R. Cammi, J. W. Ochterski, R. L. Martin, K. Morokuma, O. Farkas, J. B. Foresman and D. J. Fox, *Gaussian 16, revision B.01*, Gaussian, Inc., Wallingford, CT, 2016.
44. (a) A. D. Becke, Density-functional thermochemistry. III. The role of exact exchange, *J. Chem. Phys.*, 1993, **98**, 5648-5652; (b) C. Lee, W. Yang and R. G. Parr, Development of the Colle-Salvetti correlation-energy formula into a functional of the electron density, *Phys. Rev. B*, 1988, **37**, 785-789.
45. S. Grimme, J. Antony, S. Ehrlich and H. Krieg, A consistent and accurate ab initio parametrization of density functional dispersion correction (DFT-D) for the 94 elements H-Pu, *J. Chem. Phys.*, 2010, **132**.
46. (a) M. Bühl and H. Kabrede, Geometries of Transition-Metal Complexes from Density-Functional Theory, *J. Chem. Theory Comput.*, 2006, **2**, 1282-1290; (b) M. Bühl, C. Reimann, D. A. Pantazis, T. Bredow and F. Neese, Geometries of Third-Row Transition-Metal Complexes from Density-Functional Theory, *J. Chem. Theory Comput.*, 2008, **4**, 1449-1459.
47. A. V. Marenich, C. J. Cramer and D. G. Truhlar, Universal Solvation Model Based on Solute Electron Density and on a Continuum Model of the Solvent Defined by the Bulk Dielectric Constant and Atomic Surface Tensions, *J. Phys. Chem. B*, 2009, **113**, 6378-6396.
48. M. Álvarez-Moreno, C. de Graaf, N. López, F. Maseras, J. M. Poblet and C. Bo, Managing the Computational Chemistry Big Data Problem: The ioChem-BD Platform, *J. Chem. Inf. Model.*, 2015, **55**, 95-103.
49. G. Jones, P. Willett, R. C. Glen, A. R. Leach and R. Taylor, Development and validation of a genetic algorithm for flexible docking, *J. Mol. Biol.*, 1997, **267**, 727-748.
50. D. J. Kissick, C. M. Dettmar, M. Becker, A. M. Mulichak, V. Cherezov, S. L. Ginell, K. P.

Battaile, L. J. Keefe, R. F. Fischetti and G. J. Simpson, Towards protein-crystal centering using second-harmonic generation (SHG) microscopy, *Acta Crystallogr., Sect. D: Biol. Crystallogr.*, 2013, **69**, 843-851.

51. I. A. Qureshi, F. Ferron, C. C. Seh, P. Cheung and J. Lescar, Crystallographic structure of ubiquitin in complex with cadmium ions, *BMC Research Notes*, 2009, **2**, 251.
52. R. Diamond, Real-space refinement of the structure of hen egg-white lysozyme, *J. Mol. Biol.*, 1974, **82**, 371-391.
53. E. F. Pettersen, T. D. Goddard, C. C. Huang, G. S. Couch, D. M. Greenblatt, E. C. Meng and T. E. Ferrin, UCSF Chimera–A visualization system for exploratory research and analysis, *J. Comput. Chem.*, 2004, **25**, 1605-1612.
54. (a) G. Sciortino, J. Rodríguez-Guerra Pedregal, A. Lledós, E. Garribba and J.-D. Maréchal, Prediction of the interaction of metallic moieties with proteins: An update for protein-ligand docking techniques, *J. Comput. Chem.*, 2018, **39**, 42-51; (b) G. Sciortino, E. Garribba and J.-D. Maréchal, Validation and Applications of Protein–Ligand Docking Approaches Improved for Metalloligands with Multiple Vacant Sites, *Inorg. Chem.*, 2019, **58**, 294-306; (c) G. Sciortino, J.-D. Maréchal and E. Garribba, Integrated experimental/computational approaches to characterize the systems formed by vanadium with proteins and enzymes, *Inorg. Chem. Front.*, 2021, **8**, 1951-1974.
55. J.-E. Sánchez-Aparicio, L. Tiessler-Sala, L. Velasco-Carneros, L. Roldán-Martín, G. Sciortino and J.-D. Maréchal, BioMetAll: Identifying Metal-Binding Sites in Proteins from Backbone Preorganization, *J. Chem. Inf. Model.*, 2021, **61**, 311-323.
56. S. C. Lovell, J. M. Word, J. S. Richardson and D. C. Richardson, The penultimate rotamer library, *Proteins: Struct., Funct., Bioinf.*, 2000, **40**, 389-408.
57. (a) J. Rodríguez-Guerra, *Insilichem/gaudiview: Pre-alpha public releas, Zenodo*, 2017; (b) J. Rodríguez-Guerra Pedregal, G. Sciortino, J. Guasp, M. Municoy and J.-D. Maréchal, GaudiMM: A modular multi-objective platform for molecular modeling, *J. Comput. Chem.*, 2017, **38**, 2118-2126.
58. E. Garribba, G. Micera, D. Sanna and L. Strinna-Erre, The Cu(II)-2,2'-bipyridine system revisited, *Inorg. Chim. Acta*, 2000, **299**, 253-261.
59. K. W. H. Stevens, The Spin-Hamiltonian and Line Widths in Nickel Tutton Salts, *Proc. Roy. Soc. of London, Ser. A.*, 1952, **214**, 237-246.
60. D. Arias-Zárate, M. F. Ballesteros-Rivas, R. A. Toscano and J. Valdés-Martínez, Crystal structure of di-μ-hydroxido-bis[aqua(1,10-phenanthroline-κ^2-*N*,*N*′)copper(II)] naphthalene-2,6-dicarboxylate hexahydrate, *Acta Crystallogr., Sect. E: Cryst. Commun.*, 2015, **71**, 360-362.

61. B. D. Liboiron, K. H. Thompson, G. R. Hanson, E. Lam, N. Aebischer and C. Orvig, New Insights into the Interactions of Serum Proteins with Bis(maltolato)oxovanadium(IV): Transport and Biotransformation of Insulin-Enhancing Vanadium Pharmaceuticals, *J. Am. Chem. Soc.*, 2005, **127**, 5104-5115.
62. (a) D. Sanna, G. Micera and E. Garribba, New Developments in the Comprehension of the Biotransformation and Transport of Insulin-Enhancing Vanadium Compounds in the Blood Serum, *Inorg. Chem.*, 2010, **49**, 174-187; (b) D. Sanna, P. Buglyo, G. Micera and E. Garribba, A quantitative study of the biotransformation of insulin-enhancing VO^{2+} compounds, *J. Biol. Inorg. Chem.*, 2010, **15**, 825-839; (c) D. Sanna, G. Micera and E. Garribba, Interaction of VO^{2+} Ion and Some Insulin-Enhancing Compounds with Immunoglobulin G, *Inorg. Chem.*, 2011, **50**, 3717-3728; (d) D. Sanna, L. Biro, P. Buglyo, G. Micera and E. Garribba, Biotransformation of BMOV in the presence of blood serum proteins, *Metallomics*, 2012, **4**, 33-36; (e) D. Sanna, G. Micera and E. Garribba, Interaction of Insulin-Enhancing Vanadium Compounds with Human Serum holo-Transferrin, *Inorg. Chem.*, 2013, **52**, 11975-11985.
63. (a) V. Katta and B. T. Chait, Observation of the heme-globin complex in native myoglobin by electrospray-ionization mass spectrometry, *J. Am. Chem. Soc.*, 1991, **113**, 8534-8535; (b) L. Konermann, F. I. Rosell, A. G. Mauk and D. J. Douglas, Acid-Induced Denaturation of Myoglobin Studied by Time-Resolved Electrospray Ionization Mass Spectrometry, *Biochemistry*, 1997, **36**, 6448-6454; (c) Y. Konishi and R. Feng, Conformational Stability of Heme Proteins in vacuo, *Biochemistry*, 1994, **33**, 9706-9711.
64. A. Varshavsky, in *Encyclopedia of Genetics*, ed. J. H. Miller, Academic Press, New York, 2001, pp. 2091-2093.
65. E. de Hoffmann and V. Stroobant, *Mass Spectrometry Principles and Applications, Third Edition*, John Wiley & Sons Ltd., Chichester, 2007.
66. (a) G. Sciortino, D. Sanna, V. Ugone, J.-D. Maréchal, M. Alemany-Chavarria and E. Garribba, Effect of secondary interactions, steric hindrance and electric charge on the interaction of $V^{IV}O$ species with proteins, *New J. Chem.*, 2019, **43**, 17647-17660; (b) A. Banerjee, S. P. Dash, M. Mohanty, G. Sahu, G. Sciortino, E. Garribba, M. F. N. N. Carvalho, F. Marques, J. Costa Pessoa, W. Kaminsky, K. Brzezinski and R. Dinda, New V^{IV}, $V^{IV}O$, $V^{V}O$, and $V^{V}O_2$ Systems: Exploring their Interconversion in Solution, Protein Interactions, and Cytotoxicity, *Inorg. Chem.*, 2020, **59**, 14042-14057; (c) J. Costa Pessoa, M. F. A. Santos, I. Correia, D. Sanna, G. Sciortino and E. Garribba, Binding of vanadium ions and complexes to proteins and enzymes in aqueous solution, *Coord. Chem. Rev.*, 2021, **449**, 214192.
67. K. Strupat, in *Methods Enzymol.*, Academic Press, 2005, pp. 1-36.

68. V. Ugone, D. Sanna, G. Sciortino, D. C. Crans and E. Garribba, ESI-MS Study of the Interaction of Potential Oxidovanadium(IV) Drugs and Amavadin with Model Proteins, *Inorg. Chem.*, 2020, **59**, 9739-9755.
69. G. Ferraro, M. Paolillo, G. Sciortino, E. Garribba and A. Merlino, Multiple and Variable Binding of Pharmacologically Active Bis(maltolato)oxidovanadium(IV) to Lysozyme, *Inorg. Chem.*, 2022, **61**, 16458-16467.
70. G. Ferraro, G. Tito, G. Sciortino, E. Garribba and A. Merlino, Stabilization and binding of $[V_4O_{12}]^{4-}$ and unprecedented $[V_{20}O_{54}(NO_3)]^{n-}$ to lysozyme upon loss of ligands and oxidation of the potential drug $V^{IV}O$(acetylacetonato)$_2$, *Angew. Chem., Int. Ed.*, 2023, **62**, e202310655.
71. G. Ferraro, E. Garribba and A. Merlino, Exploring polyoxidovanadate–protein interaction, *Trends in Chemistry*, 2025, **7**, 3-6.
72. G. Tito, G. Ferraro, F. Pisanu, E. Garribba and A. Merlino, Non-Covalent and Covalent Binding of New Mixed-Valence Cage-like Polyoxidovanadate Clusters to Lysozyme, *Angew. Chem., Int. Ed.*, 2024, **63**, e202406669.
73. D. Sanna, V. Ugone, M. Serra and E. Garribba, Speciation of potential anti-diabetic vanadium complexes in real serum samples, *J. Inorg. Biochem.*, 2017, **173**, 52-65.
74. P. Nunes, I. Correia, F. Marques, A. P. Matos, M. M. C. dos Santos, C. G. Azevedo, J.-L. Capelo, H. M. Santos, S. Gama, T. Pinheiro, I. Cavaco and J. Costa Pessoa, Copper Complexes with 1,10-Phenanthroline Derivatives: Underlying Factors Affecting Their Cytotoxicity, *Inorg. Chem.*, 2020, **59**, 9116-9134.

Data availability statement

The data supporting this article have been included as part of the Electronic Supplementary Information.